# CORRELATING LABORATORY CONDITIONING AND FIELD PERFORMANCE IN PERMEABLE FRICTION COURSE ASPHALT MIXTURES

A Thesis

by

RYAN ALEXANDER HILL

Submitted to the Office of Graduate and Professional Studies of
Texas A&M University
in partial fulfillment of the requirements for the degree of

MASTER OF SCIENCE

| | |
|---|---|
| Chair of Committee, | Amy Epps Martin |
| Committee Members, | Dallas Little |
| | Bruce Herbert |
| Head of Department, | Robin Autenrieth |

December 2015

Major Subject: Civil Engineering

## ABSTRACT

Permeable Friction Course (PFC) is a type of hot mix asphalt (HMA) mixture designed to allow water to freely flow through it. PFC is used as a surface course on high-speed roadways to reduce standing water and eliminate hydroplaning. Additional benefits include improved visibility, safety, and driver comfort. Despite its many benefits the material is plagued by a shorter service life than dense-graded HMA due to its susceptibility to moisture damage which manifests through its primary pavement distress – raveling. The objective of this study was to recommend PFC laboratory testing and conditioning protocols to simulate field performance. These protocols are intended to be used in forensic analysis and to evaluate PFC mix design procedures.

Morphological and physiochemical properties of asphalt mixture component materials were examined to reveal the component materials propensity for moisture susceptibility. Volumetrics, binder stiffness, aggregate morpholgy, and surface energy were evaluated. Compacted specimens of six asphalt mixtures were tested using the Hamburg-Wheel Tracking Test and a single conditioning protocol was used to evaluate the effect of moisture conditioning on IDT strength and Cantabro Loss. Test results were compared to previous observations of the field performance of laboratory mixtures to validate the testing and conditioning protocols. High variability of test results led to only one test, the Cantabro Loss test, being recommended to predict field performance. A laboratory

conditioning protocol was not recommended as the experimental protocol did not induce sufficient moisture damage to significantly impact test results.

## DEDICATION

This work is dedicated to my beautiful wife, Janel, and

my children, Madelyn, Bryson, Carter, and Baby #4,

whose love and support have provided me with all of the inspiration I will ever need to persevere through life's many trials.

## ACKNOWLEDGEMENTS

I must first give thanks to my committee chair, Dr. Amy Epps Martin, without whose wisdom, constructive guidance and bridge-crossing acumen I would never have completed this research. Her courage and strength in the face of adversity served as a lesson that extended far beyond the scope of this research. Thank you as well to my committee members, Dr. Dallas Little, and Dr. Bruce Herbert, for their insightful comments, encouragement, and guidance.

I would like to extend my gratitude to Dr. Edith Arambula, associate research engineer and principal investigator on the FDOT project, for her constant support, guidance, and knowledge. Thank you for always having an open door and an encouraging word - no matter the test results.

Many thanks to Rick Canatella and Tony Barbosa, research technicians at the Texas Transportation Institute McNew Lab, as their expertise with the experiments and their efforts to make sure I always had the equipment and supplies I needed ensured the success of my work. Thank you as well to Dr. Emad Kassem, for his assistance with the Wilhelmy Plate testing and Dr. Eun Sug Park, for her help with the statistical analysis of the experimental data.

Thank you to my friends and colleagues for their friendship and intellect. A special thank you to Fan for generally being the smartest person in the room and for always being willing to help. Thank you to Lorena, Josh, Juan, and Charles for providing wise counsel and the small nudges that helped keep me on track.

Thank you to the United States Air Force for providing me with the marvelous opportunity to pursue my passion for knowledge and for providing numerous opportunities over the years with which to apply it.

I would also like to thank my mother and father for instilling in me the desire to understand the many “why’s” in life and never settling to tell me “just because.” Thank you to my three beautiful children, Madelyn, Bryson, and Carter, for always providing a restorative break from my work and a little bit of perspective. Finally, my sincerest appreciation goes to my wife, Janel, without whom this effort wouldn’t have been possible. Thank you for the countless times you have put our family before yourself, and thank you for your support, your patience, and most of all, your love.

## NOMENCLATURE

| | |
|---|---|
| HMA | Hot-Mixed Asphalt |
| OGFC | Open-Graded Friction Course |
| PFC | Permeable Friction Course |
| NCHRP | National Cooperative Highway Research Program |
| DOT | Department of Transportation |
| LMLC | Laboratory Mixed Laboratory Compacted |
| STOA | Short-Term Oven Age |
| IDT | Indirect Tensile Strength |
| HWTT | Hamburg Wheel-Track Testing |
| PG | Performance-Graded |
| SGC | Superpave Gyratory Compactor |
| SIP | Stripping Infection Point |
| DSR | Dynamic Shear Rheometer |
| $G_{mm}$ | Maximum Theoretical Specific Gravity |
| $G_{mb}$ | Bulk Specific Gravity |
| ANOVA | Analysis of Variance |
| SFE | Surface Free Energy |
| G* | Complex Modulus |

**TABLE OF CONTENTS**

Page

## LIST OF FIGURES

Page

## LIST OF TABLES

Page

# 1. INTRODUCTION

Permeable or Porous Friction Course (PFC), also known as Open-graded Friction Course (OGFC), is a type of asphalt mixture that has been used throughout North America and Europe for over 50 years (*1*). The basic design of PFC requires a highly open-graded aggregate gradation, high asphalt binder content, and high air voids content (typically above 18 percent) (*2*). These qualities provide for a permeable medium that allows water to flow freely through the asphalt mixture. The porous nature of the asphalt mixture reduces or eliminates standing water on the road surface thus reducing hydroplaning and splash/spray while improving surface friction and wet weather visibility of pavement markings. The abundant air voids also serve to decrease tire/pavement noise and provide a filter mechanism to improve the quality of stormwater runoff (*3*). Though PFC is still used in the low-volume roads and parking lots it was originally designed for, its primary use today is on high traffic roadways at highway speeds.

These demanding conditions require a durable mix design. A new generation of PFC utilizing polymer-modified asphalt binders, higher asphalt binder contents, and asphalt binder additives has become the norm (*2; 3*). Despite the use of improved materials and construction techniques, the open nature of PFC leads to the early and often rapid onset of several pavement distresses. The most prevalent distress in PFC is raveling which occurs when aggregate particles dislodge from the pavement surface (*1-4*).

Included in this thesis is a history and background of PFC which frames the problem statement and research objective. The literature review presents a background on moisture damage and highlights research which provided the necessary context to establish the research objective. The next section is the materials and experiment design which discusses how materials were chosen for testing and what component material properties were investigated. The experiment design provides a description of the specimen fabrication protocol as well as details of all of the mixture tests executed. The results and analysis section presents the results of the component material and performance tests. The effectiveness of the moisture conditioning protocol is analyzed and discussion on the significance of all test results is provided. Conclusions are then presented and recommendations are made for future research. Finally, references are provided for all in-text citations.

### 1.1 History

The beginnings of PFC can be traced to early applications of plant mix seal coats by the California Department of Highways in the 1940s. California was looking for alternatives to chip seals and slurry seals as they were having problems with friction loss, aggregate de-bonding, and construction limitations. These early plant mix seal coats provided greatly improved friction characteristics and ride quality as compared to chip and slurry seals (*1; 3*). Many western states adopted these improved seal coats over the following decades, but their use remained limited due to durability and draindown issues. Draindown was generally due to the high asphalt binder content and uniform gradation

of the early seal coat mixtures, which allowed the asphalt binder to drain off the aggregate creating a thin film thickness and making the asphalt mixture more prone to raveling. More states began using the plant mix seal coats during the 1970s due to an FHWA initiative to improve the friction characteristics of U.S. roadways. A 1978 FHWA report officially named these asphalt mixtures OGFC and the first OGFC mix design was published in 1980 (*3*). Though the draindown and durability issues of OGFC continued throughout the 1980s, the use of OGFC increased by 80% from 1978 to 1988 (*1*). Figure 1 shows the use of OGFC in the United States and is adapted from two surveys, one from NCHRP Synthesis 284 and one from NCHRP Report 640 (*1; 3*).

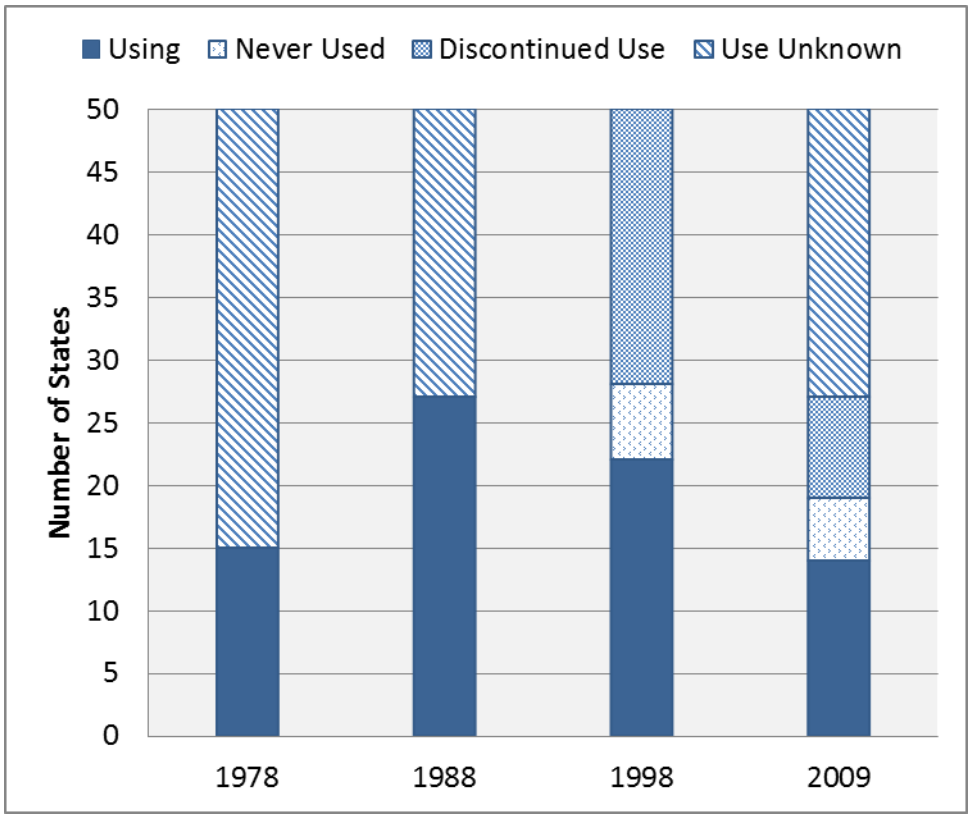


**FIGURE 1 History of OGFC in the U.S. (Adapted from (*1; 3*)).**

In the early 1990s, the Georgia Department of Transportation (GDOT) began the testing and limited use of what would become the newest generation of OGFC. Taking inspiration from recently developed Porous European Mix (PEM), GDOT began adding hydrated lime to their OGFC mixture as an anti-stripping agent. They also added fibers to prevent draindown of the asphalt binder. Newly developed polymer-modified asphalt binders were used to improve durability. In addition, production temperatures were increased to provide drier aggregates which were thought to improve aggregate-asphalt binder adhesion. Finally, coarser gradations and thicker layers were used to improve permeability (*5*). A 1998 survey of state DOTs by the National Center for Asphalt Technology (NCAT) revealed that many states were reporting good performance from OGFC mixtures after adopting the coarser gradations, modified asphalt binders, and stabilizing additives of GDOT (*6*). After this survey, NCAT developed a mix design procedure for the new-generation of OGFC now known as PFC (*3*).

### 1.2 Definition

PFC is an open-graded asphalt mixture (see Figure 2) with interconnected air voids that allows water to flow through it during rain events. It is typically used as a surface or wearing course no more than 2 inches thick. Placed above a layer of impermeable material (typically a dense-grade hot-mix asphalt (HMA) layer), water drains vertically through the PFC then laterally away from centerline to the exposed pavement edge (*2*).

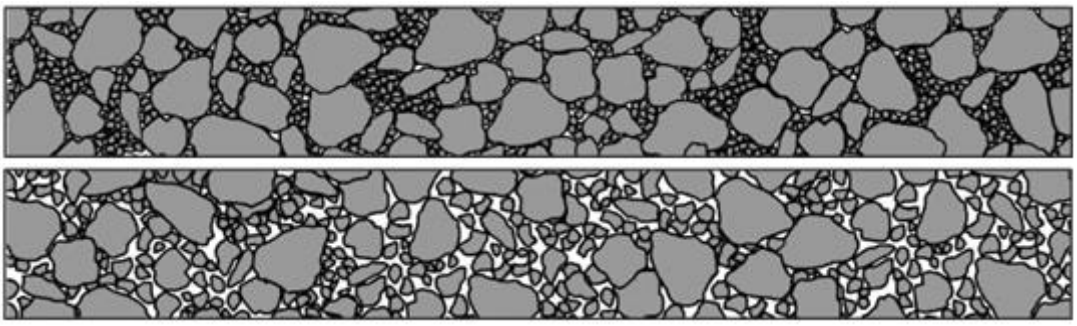

**FIGURE 2 Comparison of Dense Graded HMA (top) vs. PFC (bottom) (7).**

### 1.3 Benefits

The open structure of PFC has been shown to have many functional benefits. These benefits can be categorized into two key areas: safety and environmental. The safety benefits of PFC are well documented and are the result of two main features of the asphalt mixture, its permeability and the surface macro-texture. These features reduce hydroplaning, splash/spray, and light reflection while improving skid resistance and wet weather friction. Hydroplaning occurs when a layer of standing water breaks the contact between the tire and the pavement surface at high speeds (*3*). In PFC, during a heavy rainfall, water flows through the surface layer and thus standing water is removed from the surface. The absence of standing water eliminates hydroplaning, and splash/spray may be reduced up to 95% as compared to dense-graded asphalt mixtures (*2*). Several references in the United States and Europe indicated that the increased macro-texture of PFC contributes to improved wet weather friction as well (*3*).

Perhaps of primary importance, these safety benefits have led to a marked decrease in wet weather accidents. Cooley et al. (*3*) reported that research in Virginia, France, Canada, and Japan showed that PFC layers reduced wet weather accidents. Rand (*8*) reported that after PFC was placed on a section of RM1431 in Texas, wet weather accidents dropped from a yearly average of 21.3 to just over 1 in the three years before and after placement, respectively. This remarkable drop in accidents occurred even as the number of wet weather days *increased* after placement of the PFC section.

Some of the environmental advantages of PFC are increased smoothness, improved water quality of stormwater runoff, and a reduction in tire/pavement noise. The improved smoothness has been linked by several researchers to increased fuel economy (*3*). Barrett and Stanard found in their 40-month study of a roadway in Texas that PFC reduced Total Suspended Solids (TSS), total metals, and total phosphorous by as much as 93%. This study was unique in that the sites evaluated had both PFC and standard HMA in the same location thus reducing variability in environmental conditions. Perhaps the most well researched environmental benefit is the reduction in tire/pavement noise. Numerous studies indicated that the high air void structure of PFC led to noise reductions on average of 3 dB(A) as compared to dense-graded HMA at highway speeds (*1-3; 9*). This noise reduction is equivalent to reducing the traffic volume by half or doubling the distance of the noise receiver from the road. As these two solutions are typically not achievable on most major roadways, the noise reduction capabilities of PFC are highly valued. Kandhal (*2*) presented an interesting perspective by noting that the

construction of noise barriers along highways is done at a cost of $15 to $20 per linear foot with an anticipated noise reduction of 3-5 dB(A) – roughly equivalent to using a PFC, but with a much higher cost.

### 1.4 Limitations

While the functional benefits of PFC have been well accepted, the durability of the material has consistently been a top concern of government agencies and researchers. As was previously discussed, raveling is the main distress seen in PFC pavements (*1-4*) and thus its causes are the main factors affecting the durability of PFC. An example of raveling in a Florida PFC is shown in Figure 3.

**FIGURE 3 Raveling of Florida PFC (*10*).**

Raveling occurs at the surface of PFC in the short-term and in the long-term (*11*). Short-term raveling occurs due to high shear forces from tire/pavement interaction and may be the result of poor construction practices. Long-term raveling is the result of draindown, where gravity combined with high temperatures and high asphalt binder content cause the asphalt binder to drain off the aggregate. This leaves the aggregate with a reduced film thickness and thus more exposure to the elements and more prone to stripping (*11*). Another theory that has been presented to explain the occurrence of raveling is the failure of one or a combination of the adhesive bond between the aggregate and the asphalt binder and the cohesive strength of the asphalt binder itself. In all cases, aging and the subsequent embrittlement of exposed asphalt binder in the open-graded pavement structure is also a contributing factor (*12*). The mechanical forces present at the pavement surface under traffic then initiate raveling. As material is dislodged and new material exposed to the abrasive shear forces of tires, raveling quickly progresses across the pavement surface.

### 1.5 Problem Statement

The use of PFC on roadways improves motorist safety, increases driver comfort, and provides several environmental advantages. These benefits do not come without a cost as the typical service life of PFC is only 8-10 years (*3*) while a standard hot mix asphalt (HMA) road may remain in service in excess of 20 years (*13*). The primary distress that causes this reduction in PFC service life is raveling. While raveling is commonly seen in

PFC applications, a stronger correlation between laboratory testing and field performance is needed to design more durable asphalt mixtures.

### 1.6 Research Objective

While some research has been conducted on PFC mix design and laboratory testing and conditioning to evaluate asphalt mixture durability, there has been limited research relating laboratory characterization and field performance. The goal of this study is to recommend laboratory testing and conditioning to induce PFC asphalt mixture degradation and simulate field conditions for use in evaluation during mix design or forensic analysis.

# 2. LITERATURE REVIEW

This section contains the results of a literature review of research used to develop the research objective and experimental design. A background of research on moisture damage and understanding the moisture susceptibility of asphalt mixtures is provided. An explanation of the importance of Surface Free Energy (SFE) and its relevance to the ability of PFC to resist moisture damage is also discussed. Finally, an examination of research specifically related to PFC mixtures was conducted. Particular emphasis was placed on research and field observations regarding the durability of PFC mixtures and laboratory conditioning - including both aging and moisture conditioning – and its correlation to raveling in the field.

## 2.1 Background on Moisture Damage

Moisture enters an asphalt pavement system in several ways. Precipitation at the surface of the asphalt mixture can be forced through the pavement structure by gravity or the hydraulic pressure from tires (*14*). This is particularly the case in PFC where the surface course is specifically designed to transport water through the asphalt mixture. Moisture can also move through an asphalt pavement through capillary rise from the subgrade or unbound aggregate layers. This may be exacerbated in PFC where the presence of debris can clog the open-graded structure trapping moisture in the impermeable asphalt pavement underlayer (*1*). Whatever the mode of water transport, the subsequent interaction of asphalt binder, aggregate, and water within the pavement structure is a

complex phenomenon. Combined with the repetitive loading of traffic, the moisture-related distresses caused by this interaction are an issue in asphalt pavements nationwide. A 2002 AASHTO survey of 55 transportation agencies found that 82% of respondents had to treat their pavements for moisture damage (*15*). Moisture damage is best defined by Kiggundu and Roberts as "the progressive functional deterioration of a pavement mixture by loss of adhesive bond between asphalt cement and the aggregate surface and/or loss of the cohesive resistance within the asphalt cement principally from the action of water" (*16*).

Moisture damage may manifest in several forms of pavement distress. The most common distresses as presented by Caro et al. (*17*) are raveling, stripping, shelling, and hydraulic scour. Raveling was defined in the previous section, and stripping is the physical separation of aggregate and asphalt binder due to the loss of adhesion at the interface of these materials in the presence of moisture. Shelling is the loosening and removal of aggregate from a seal coat or other surface treatment. Hydraulic scouring occurs as saturated surfaces of pavement material are eroded due to the dynamic action of tires in the presence of water. Hicks et al. (*15*) also mention bleeding, rutting, and cracking as moisture-related distresses. In the case where moisture is not the primary degrading factor initiating a distress, moisture may contribute - if not accelerate - the progression of these distresses in combination with other factors (materials, design, construction).

The adhesive bond between the aggregate and the asphalt binder will provide a key focus in this research and the importance of stripping, or the loss of that bond, is of primary concern to examine moisture conditioning of PFC in the laboratory. It is therefore useful to examine the mechanisms of moisture damage, particularly as they relate to stripping. Little and Jones (*18*) provide a thorough explanation of those mechanisms in their 2003 paper for the national seminar on moisture susceptibility of asphalt pavements. Those mechanisms are summarized in Table 1 and presented in the following paragraphs in further detail.

**TABLE 1 Adhesive and Cohesive Failure Mechanisms Associated with Moisture Damage (*14*)**

| Mechanism | Adhesion | Cohesion |
|---|---|---|
| Detachment | ● | |
| Displacement -Film Rupture | ● | |
| Spontaneous Emulsification | | ● |
| Pore Pressure | ● | ● |
| Hydraulic Scour | ● | |
| pH Instability | ● | |
| Environmental Factors | ● | ● |

**Detachment** is the separation of an asphalt binder film from an aggregate surface by a thin film of water without an obvious break in the film. It is thought to be caused by the

incomplete drying of aggregate during asphalt mixture production (*19*). **Displacement** is similar to detachment except that the separation of asphalt binder from the aggregate surface occurs because of a break in the asphalt film. This may occur due to a break in the asphalt film or film rupture. Several factors - involving the SFE of the asphalt binder and aggregate - that provide a more thorough understanding of the rationale for detachment and displacement will be discussed subsequently. Figure 4 provides an illustration of the loss of bond at the aggregate-asphalt binder interface in detachment and displacement.

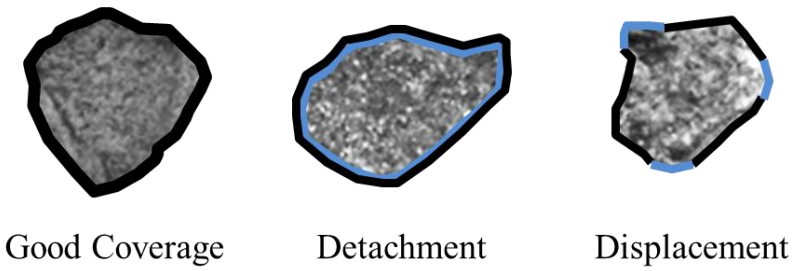


**FIGURE 4 Comparison of Loss of Adhesion (Adapted from (*20*)).**

**Spontaneous Emulsification** is an inverted emulsion where water droplets form in the asphalt binder. This mechanism is unique in that it leads to cohesive failure in the asphalt binder. **Pore Pressure** can build in water trapped in the asphalt mixture during repeated traffic loadings. This can lead to a densification or hardening of the asphalt binder which may lead to strengthening or microcracking. This may reduce the cohesive strength of the asphalt binder. In addition, a build-up of pore pressure may disrupt the asphalt binder film which may lead to adhesive failure of the aggregate-asphalt binder

interface (*18*). **Hydraulic Scour** occurs at the pavement surface as water is sucked under the tire and into the pavement by the tire action. Stripping results from the abrasive action of tires on a saturated surface (*18*). **pH Instability** refers to the fact that the aggregate-asphalt binder bond is strongly influenced by the pH of the contact water and that stabilizing the pH sensitivity at the aggregate-asphalt binder interface can reduce stripping (*16*). Temperature, air and water exposure, and severe weather (namely freeze/thaw) are all **Environmental Factors** that have a considerable effect on the durability of asphalt mixtures and the strength of the aggregate-asphalt binder bond.

Given the prevalence of moisture damage in asphalt pavements and the complexity of the mechanisms which cause it, testing to evaluate the moisture susceptibility of asphalt mixtures and their components is important. The 2002 AASHTO survey found that 87% of the 55 surveyed agencies conduct some form of test for moisture susceptibility (*15*). Several researchers have presented comprehensive summaries of the history and state-of-the-practice of testing for moisture susceptibility (*14; 17; 21; 22*). As the focus of this research was on the use of two specific tests for laboratory conditioning, the full details of every available test will not be presented here, though a brief summary is provided.

Researchers have studied the adverse effects of moisture on asphalt pavements since the 1920s. Since that time many tests have been developed and they can be divided into two main categories: qualitative (providing a subjective evaluation of stripping potential) and quantitative (providing a value for a specific parameter – such as strength before and

after conditioning). The tests may also be divided into tests to determine the compatibility of aggregate and asphalt binder using loose mixtures and tests to evaluate the moisture susceptibility of compacted specimens (*22*). Santucci (*14*) presents a third category of tests which evaluate the compatibility of individual components before mixing.

Table 2 summarizes, the four criteria provided by Solaimanian et al. (*22*) for a moisture susceptibility test to be successful for asphalt mixture design and field performance evaluation.

**TABLE 2 Criteria for Tests to Successfully Identify Moisture Susceptibility (*22*)**

| | |
|---|---|
| 1 | Must be representative of the mechanisms that cause moisture damage in the field an produce results that match field results. |
| 2 | Must be capable of discriminating between poor and good performers in regards to stripping. |
| 3 | Must be repeatable and reproducible |
| 4 | Must be feasible, practical and economical enough to use in routine practice. |

Of the moisture susceptibility tests conducted on compacted specimens, nearly all involve the quantitative comparison of specimens before and after conditioning. The 2002 AASHTO survey found that 85% of respondents used the tensile strength ratio (TSR) of indirect tensile (IDT) strength before and after some conditioning protocol as

their evaluation parameter for moisture susceptibility. The TSR is illustrated in Figure 5. The most widely used test on compacted specimens is the modified Lottman Test or AASHTO T283. 72% of agencies used AASHTO T283 or the original Lottman conditioning protocol to evaluate the moisture susceptibility of their pavements. Despite the wide use of AASHTO T283, major concerns have been noted by researchers about its reproducibility and its ability to predict moisture susceptibility with reasonable confidence (*22*). The results of a 2000 NCHRP report by Epps et al. (*23*) indicated that AASHTO T283 laboratory test results did not accurately reflect moisture susceptibility of asphalt mixtures as observed in the field.

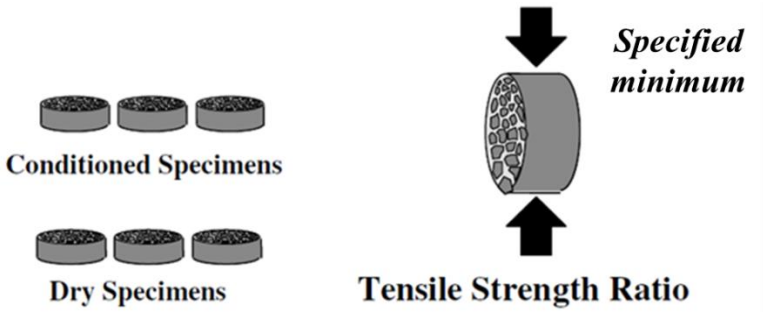


**FIGURE 5 Determining TSR Using IDT for Dry and Conditioned Specimens.**

Two other tests that are not widely used to test for moisture susceptibility, but have shown promise for more accurately correlating laboratory mixture performance to field performance, are the Hamburg Wheel Tracking Test (HWTT) and the Moisture Induced Sensitivity Test (MIST). Research from several state DOTs has shown that the HWTT and the MIST are good predictors of stripping in the field (*21; 24*). Schram et al. conducted a study using five dense-graded HMA field sections and the following five

moisture susceptibility test methods: dynamic modulus, flow number, AASHTO T283, HWTT, and MIST. The field sections were from locations with different traffic and environmental conditions. The HWTT and MIST outperformed all other tests in their prediction of acceptable field performance. Both tests were chosen for this study, and specific test procedures will be described in detail in the next section.

### 2.2 SFE and Aggregate-Asphalt Binder Bond Strength

While it is clear from the 2002 AASHTO survey that most agencies use moisture sensitivity tests designed for use on compacted specimens, it is also advantageous to know the expected compatibility of combinations of aggregate and asphalt binder when considering a proposed mix design's resistance to moisture damage in the field. This information would allow materials and design engineers to make adjustments to the selected components and additives in a mix design in conjunction with the asphalt mixture characterization. The use of SFE measurements of the individual aggregate and asphalt binder may provide that capability. The following discussion on SFE is adapted extensively from Bhasin et al. (*25*), Little and Jones (*18*), and Little and Bhasin (*26*).

SFE ($\gamma$ in ergs/cm$^2$) is a fundamental material property defined as the work required to create a new unit area of surface of a material. Acid-Base theory divides the total SFE into three components: a non-polar or dispersive component known as the Lifshitz-van der Waals (LW) component, the Lewis acid component, and the Lewis base component. The total surface free energy of a material is represented as follows:

$$\gamma^{\text{total}} = \gamma^{\text{LW}} + \gamma^{+-} = \gamma^{\text{LW}} + 2\sqrt{\gamma^{+}\gamma^{-}} \quad (1)$$

Where:

$\gamma$ = total surface free energy of the material

$\gamma^{LW}$ = LW component

$\gamma^{+-}$ = acid-base component

$\gamma^{+}$ = Lewis acid component

$\gamma^{-}$ = Lewis base component

When the SFE components of two materials are known, Equation 2 can be used to determine the work of adhesion between those materials:

$$W_{\text{AB}} = 2\sqrt{\gamma_{\text{A}}{}^{\text{LW}}\gamma_{\text{B}}{}^{\text{LW}}} + 2\sqrt{\gamma_{\text{A}}{}^{+}\gamma_{\text{B}}{}^{-}} + 2\sqrt{\gamma_{\text{A}}{}^{-}\gamma_{\text{B}}{}^{+}} \quad (2)$$

where, in an asphalt mixture, the subscripts A and B represent the aggregate and asphalt binder, respectively. For an aggregate to be durable and resistant to moisture damage, the work of adhesion between the aggregate and asphalt binder, $W_{AB}$, should be as high as possible. A higher magnitude of work of adhesion means that it takes more work to separate the asphalt binder from the aggregate surface (*25*).

In a three-phase system (as in the presence of moisture in an asphalt pavement) water is represented by the subscript, W. According to Little and Jones (*18*) water reduces the

free energy of the three-phase system more than asphalt, which produces a more thermodynamically favorable condition of minimum surface energy. This means that aggregate has a strong preference for water over asphalt binder. When water displaces asphalt binder from the aggregate surface, as in Figure 6, the work of debonding, $W_{ABW}^{wet}$, is determined using Equation 3:

$$W_{ABW}^{wet} = \gamma_{AW} + \gamma_{BW} - \gamma_{AB} \quad (3)$$

where the subscripts AW, BW, and AB represent the interfacial energy between the aggregate and water, asphalt binder and water, and aggregate and asphalt binder, respectively. The work of debonding can also be thought of as the reduction in free energy of the system when water displaces asphalt from the aggregate surface. A higher magnitude of $W_{ABW}^{wet}$ indicates a high thermodynamic potential for water to cause debonding, therefore it is desirable that this quantity be as small as possible to reduce moisture sensitivity (*25*).

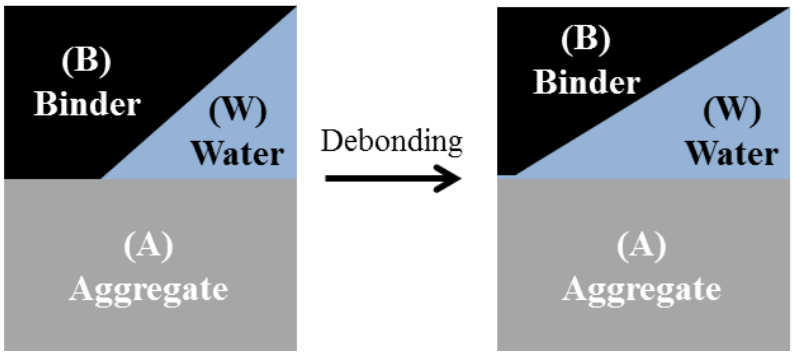


**FIGURE 6 Displacement of Asphalt Binder from Aggregate-Asphalt Binder Interface by Water (*26*).**

The interfacial energy between any two materials, i and j, is calculated using each material's SFE components from the relationship given in Equation 4:

$$\gamma_{ij} = \gamma_i + \gamma_j - 2\sqrt{\gamma_i^{LW}\gamma_j^{LW}} - 2\sqrt{\gamma_i^{+}\gamma_j^{-}} - 2\sqrt{\gamma_i^{-}\gamma_j^{+}} \quad (4)$$

The work of cohesion, $W_{BB}$, can be defined as the amount of work required to separate a column of liquid (or solid) in two and is given by Equation 5. This component plays an important role to consider in the loss of cohesion and degradation of the asphalt binder in the presence of water.

$$W_{BB} = 2\gamma_B \quad (5)$$

Equations 1 through 5 provide for the calculation of the three quantities needed to evaluate the thermodynamic potential of the aggregate-asphalt binder mixture in the presence of water; $W_{AB}$, the work of adhesion between the aggregate and the asphalt binder; $W_{ABW}^{wet}$, the work of debonding of that system in the presence of water; and $W_{BB}$, the work of cohesion of the asphalt binder. Four additional energy parameters, which combine these quantities, provide for an enhanced method to assess an asphalt mixture's susceptibility to moisture damage.

The ratio of the work of adhesion to the work of debonding is the first energy parameter, $ER_1$, and it is directly proportional to the moisture resistance of an asphalt mixture. Combinations of binders that produce a higher value of $ER_1$ are less sensitive to moisture (*26*).

$$\mathrm{ER}_1 = \left|\frac{W_{AB}}{W_{ABW}^{wet}}\right| \tag{6}$$

An important factor not considered in $ER_1$ is the wettability of an aggregate by the asphalt binder. Wettability refers to the ability of one material to wet the surface of another material. It also refers to the ability of a material to penetrate into the microtextural surface of another material. Therefore, an asphalt binder with better wettability has a stronger affinity to coat the surface of an aggregate than an asphalt binder with lower wettability. A higher wettability value allows for fewer "weak points" at the aggregate-asphalt binder interface and thus a lower susceptibility to moisture damage (*26*). $ER_2$ is the ratio of the wettability of the aggregate by the asphalt binder to the magnitude of the work of debonding and is given by Equation 7. Again, a higher value of $ER_2$ would suggest that the combination of aggregate and asphalt binder would be less sensitive to moisture.

$$\mathrm{ER}_2 = \left|\frac{W_{AB}-W_{BB}}{W_{ABW}^{wet}}\right| \tag{7}$$

Given the energy parameters, $ER_1$ and $ER_2$, it is necessary to consider the surface area of an aggregate. A higher surface area will provide a larger overall area over which the asphalt binder may bond with the aggregate. In addition, a higher specific surface area would mean a greater microtexture on the aggregate surface and a greater contact area for the aggregate-asphalt binder bond (*25*). The two energy parameters are therefore modified in Equations 8 and 9 to account for the surface area over which the asphalt binder may bond with the aggregate using the specific surface area of the aggregate.

$$\mathrm{ER}_1 \times \mathrm{SSA} = \left|\frac{W_{AB}}{W_{ABW}^{wet}}\right| \times \mathrm{SSA} \tag{8}$$

$$\mathrm{ER}_2 \times \mathrm{SSA} = \left|\frac{W_{AB}-W_{BB}}{W_{ABW}^{wet}}\right| \times \mathrm{SSA} \tag{9}$$

In summary, the SFE components of an aggregate and asphalt binder can be obtained through laboratory testing. The SFE components can be combined using thermodynamic principles to calculate four energy parameters: $ER_1$, $ER_2$, $ER_1$ * SSA, and $ER_2$* SSA. These energy parameters have been shown to be an effective tool to use in selecting materials which will be resistant to moisture damage in the field (*26*).

### 2.3 Previous Research on PFC

While many studies have been conducted investigating the susceptibility of asphalt mixtures to moisture damage, most of this research has been conducted on dense-graded

HMA while there has been less research that has focused specifically on PFC. Given that PFC is, by its functional nature, designed to be exposed to water, the ability to accurately predict its response to the environment is crucial. To better understand PFC field performance, laboratory testing, and conditioning protocols; research considering the durability of PFC and the factors that influence PFC durability was examined. In addition, several studies on moisture conditioning were examined to determine the most effective laboratory conditioning protocol.

### *2.3.1 Durability of PFC and its Influencing Factors*

To simulate in the laboratory the onset of raveling and the effects of exposure to moisture and oxygen in the field, several tests have been widely recommended and used in PFC research. The Cantabro Loss test is the most widely recommended, while determining the TSR for IDT strength for dry and unconditioned specimens is also common.

Alvarez et al. (*27*) evaluated several PFC asphalt mixture durability tests to recommend a durability test for PFC mix design to improve laboratory performance evaluations and aid in the determination of Optimum Asphalt Content (OAC) in volumetric mix design. The Cantabro Loss test, HWTT, and Overlay Test (OT) were evaluated. Laboratory Mixed Laboratory Compacted (LMLC) specimens were prepared using two asphalt binder types, one modified with a polymer and one with asphalt rubber. Nine asphalt mixtures were evaluated with specimens compacted at 18-20% air voids in the

Superpave Gyratory Compactor (SGC). HWTT and OT specimens were cut to required sizes and allowed to dry before testing, while Cantabro specimens were laboratory conditioned to produce dry, wet, low temperature, and 3 and 6 month-aged specimens. Wet specimens were conditioned for 24±0.5 hours in a water bath with a constant temperature of 60°C and then dried for 24±0.5 hours using forced ventilation at room temperature. Low temperature specimens were conditioned for 24 hours at 3°C, and aged specimens were placed in a 60°C room for the specified aging period (3 or 6 months).

Variability and a lack of clarity in the results of the HWTT and OT tests prevented recommendation of their use, but the Cantabro Loss test was recommended to evaluate durability but not as the definitive test to determine OAC. It was found that Cantabro Loss values showed a direct relationship with water-accessible AV content providing an indication of the importance of volumetric properties in PFC mix design. Further, it was shown in the Cantabro Loss test that aggregate properties have a more substantial impact on asphalt mixture performance than the asphalt binder type.

To refine the mix design process and examine several deficiencies in the design and durability of PFC mixtures, Watson et al. (*28*) conducted research on SGC compaction, mixture density and durability tests for PFC. Three aggregates typically found in PFC (granite, crushed gravel, and traprock), were combined with three different asphalt binders: an unmodified PG 67-22, a polymer modified PG 76-22, and a crumb rubber

modified PG 76-34. An analysis of $N_{design}$ levels and air void calculation methods was conducted which established that a design compaction of 50 gyrations was acceptable for these mixtures, while no recommendation could be made for the best method to determine air voids. The Cantabro Loss test was evaluated for its use with SGC specimens using asphalt mixture combinations in an unconditioned state and after aging in a forced-draft oven at 64°C for 7 days. It was shown that Cantabro Loss values decreased with increasing asphalt binder content and that the use of polymer-modified asphalt binder provided the most improvement in mixture durability. Draindown of asphalt binder was also examined, and it was determined that the addition of mineral fiber significantly reduced draindown.

Putnam (*29*) conducted research for the South Carolina DOT (SCDOT) to evaluate and compare different mix design procedures for PFC and the effect of aggregate gradation on PFC laboratory performance. After a survey of state DOTs, it was determined that PFC mix design procedures could be grouped into the following three categories: using properties of compacted specimens to determine OAC, using the absorption capacity of the aggregate to determine OAC, and using a visual inspection of loose mix to determine OAC. Specimens were fabricated for testing at different asphalt binder contents using a polymer-modified PG 76-22 asphalt binder. Hydrated lime was added at a rate of 1% by weight of aggregate, and 0.3% cellulose fiber was added by weight of mix to prevent draindown. Specimens were compacted to 50 gyrations using the SGC, and air voids were not specified but were reported from 15-21%. The Cantabro Loss test was run on

dry compacted specimens and specimens aged for 7-days at 60°C. As expected, decreased abrasion loss was seen with increasing binder content, but there was either no difference or a decrease in abrasion loss with aged specimens.

The second part of the SCDOT study evaluated the effect of aggregate gradation on PFC performance in laboratory testing. Compacted specimens were prepared for 10 aggregate gradations which produced compacted specimens with varying air voids (10%-22%) and porosity (8%-20%). The same fabrication and compaction protocols were followed using the same asphalt binder and additives as in the previous OAC study. The following laboratory tests were performed: permeability, Cantabro Loss (on unaged specimens and specimens aged at 60°C for 7 days), moisture susceptibility using TSR, and rutting resistance. It was determined that a positive correlation exists between permeability and both porosity and air voids. No correlation was found between Cantabro Loss and air voids or porosity. In addition, unaged versus aged results were inconclusive. For the moisture susceptibility test, TSR was calculated between unconditioned compacted specimens and specimens conditioned with a modified T283 protocol. It was noted that as air voids and porosity increased, the IDT strength decreased. TSR was above 80% for all asphalt mixtures, and 3 of 10 mixtures did have a TSR greater than 100%. Finally, no definitive relationship was determined between rutting and porosity or air voids.

### *2.3.2 Effect of Aging*

Hagos et al. (*12*) examined the effect of aging of asphalt binder and asphalt mixtures on PFC performance. Asphalt binder was aged in the laboratory to simulate field conditions and tested using the Dynamic Shear Rheometer (DSR) and Direct Tension Test (DTT). Field cores were evaluated using the IDT. The cores came from untrafficked sections (emergency lanes) which had been newly placed or had 1, 3, 7, or 12 years of service. Hagos determined that the two main types of failure in PFC occur due to loss of cohesive strength (within the asphalt binder) and loss of adhesive strength (between the asphalt binder and the aggregate). It was found that aging had a positive influence (through increased stiffness) at intermediate and high temperatures up to 3-4 years of service, but at low temperatures and after extended service the brittle behavior accelerated raveling. Thus, it was concluded that raveling is caused primarily due to failure in the cohesive bond within the asphalt binder and that the asphalt binder-aggregate interface contributes to, but is not the main cause of, raveling.

### *2.3.3 Moisture Conditioning*

As previously discussed, moisture sensitivity of asphalt mixtures is a well-researched field for dense-graded HMA, but studies examining the effectiveness of correlating laboratory conditioning with PFC field performance are limited. While the mechanisms and factors of moisture damage may be the same for both PFC and dense-graded HMA, it is important to evaluate the suitability of current laboratory conditioning with PFC.

Chen and Huang (*30*) evaluated the ability of several laboratory moisture conditioning protocols to induce moisture damage in dense-graded HMA specimens. Two conditioning methods were evaluated: the freeze-thaw (F-T) method of AASHTO T283 and the MIST. Specimens were prepared using three coarse gravel gradations and PG 64-22 asphalt binder with and without anti-strip additive. Laboratory moisture conditioning was conducted using the following four methods: using AASHTO T283 with one and two freeze-thaw (F-T) cycles and using the MIST at 500 and 1000 cycles. For all MIST testing a water temperature of 40°C was used with a pore pressure of 276 kPa.

Dynamic modulus, Superpave IDT creep, resilient modulus, and IDT strength tests were run on conditioned and unconditioned specimens. From these tests, they concluded that both the F-T and MIST methods effectively characterize laboratory measured moisture damage. It was also determined that an increase in the number of F-T or MIST cycles caused an increase in moisture damage. Further, the presence of an anti-strip additive reduced the amount of moisture damage in laboratory specimens.

Zofka et al. (*31*) conducted a study to evaluate the MIST as a means of accelerated moisture susceptibility testing for asphalt materials. Dense-graded WMA and HMA field cores and LMLC specimens were used. Laboratory conditioning included the standard AASHTO T283 and MIST conditioning at 60°C and 276 kpa for 3,500 cycles. After conducting IDT tests on both conditioned and unconditioned samples, it was determined

that the MIST was a viable alternative test method to AASHTO T283 for determining moisture susceptibility.

The MIST was also used in a recent study by Weldegiorgis and Tarefder (*32*) where they examined the effect of varying MIST-conditioning cycles and pressure on dynamic modulus. To that end, MIST conditioning was performed at three different temperatures (40°C, 50°C, 60°C), three different pressures (276 kPa, 379 kPa, 483 kPa), and three different numbers of cycles (3,500, 7,000, and 10,500). In each test combination, the recommended test conditions of 60°C, 276 kPa, and 3,500 cycles were used with two variables held constant (i.e. temperature and pressure) while varying the third factor (i.e. load cycles). Specimens were fabricated using PG 70-22 asphalt binder and 15% recycled asphalt pavement (RAP) and were compacted to 5.5±0.5% air voids. The dynamic modulus ratio (DMR) of wet to dry samples was measured. Testing clearly indicated the increasing trend of moisture damage with increasing MIST conditioning temperature, pressure, and cycles. Visual inspection of the samples also revealed the presence of adhesive failure between the aggregates and asphalt binder.

# 3. MATERIALS AND EXPERIMENTAL DESIGN

This section first provides an overview of the materials and mixtures used throughout this experiment as well as the laboratory testing regimen used to gather data for analysis. A review of the field sections used as performance indicators as well as their component materials and mix design is provided. Next, the tests utilized to investigate the asphalt mixture component material properties are discussed in detail. Finally, the protocols used to fabricate specimens and brief descriptions of the asphalt mixture tests are provided.

## 3.1 Selection of Materials

As the goal of this research was to tie laboratory conditioning to field performance, existing PFC road sections from the Florida Department of Transportation (FDOT) were utilized to provide materials and mix designs. Florida has used PFC since the mid-1970s to reduce the risk of hydroplaning on high speed roadways during heavy rain events. In the 1990s a more open-graded mixture, called FC-5, was adopted to further reduce hydroplaning risks (*33*). FC-5 is a ½-inch nominal maximum aggregate size (NMAS), open-graded mixture placed ¾ inches thick. Today, the FDOT Flexible Pavement Design Manual requires that FC-5 be used on all multi-lane roads with a design speed over 50mph (*34*) making its use nearly universal across high speed roadways in Florida.

### *3.1.1 Field Performance*

While FC-5 has been used for almost 20 years in Florida, durability remains an issue. FDOT has found that the average service life of FC-5 remains below that of traditional dense-graded friction course. The predominant failure mechanism in Florida's PFC is raveling and top-down cracking. While raveling has continued to be a problem, FDOT has identified and attempted to correct several common failure mechanisms associated with construction (inadequate tack coat application, long haul times, low mixture temperatures, etc.) and poor Quality Assurance/Quality Control (QA/QC) practices. To address asphalt mixture concerns, FDOT has sponsored several research projects to improve their PFC mix design (*10; 33; 35*). By providing a correlation between laboratory conditioning and field performance, this project seeks to provide FDOT a testing protocol to predict how an asphalt mixture will perform in the field. For this study, FDOT provided the mix design and materials for two "good" performing and one "poor" performing field section. Asphalt mixtures 1 and 2 were "good" performers, and asphalt mixture 3 was the "poor" performer. The bad performing asphalt mixture experienced excessive raveling early in its service life.

FDOT uses a Pavement Condition Survey to evaluate surface distresses and assess the overall condition of the pavement section. A pavement section receives a score from 0.0 (worst condition) to 10.0 (best condition) in the following three categories: cracking, rutting, and ride rating. Raveling is included in the crack rating, but has its own evaluation criteria. A rating of 6.4 or below is the trigger level for pavement

rehabilitation (*10*). The PCS raveling codes are shown in Table 3. The predominant severity level and the percent of area affected are recorded, and a raveling code is assigned to that pavement (*36*). For example, medium raveling over 20% of the pavement area would receive a value of "M2".

**TABLE 3 FDOT PCS Raveling Codes (*36*)**

| PERCENT OF PAVEMENT AREA AFFECTED BY RAVELING | RAVELING SEVERITY LEVEL AND CODE | | |
|---|---|---|---|
| | LIGHT | MODERATE | SEVERE |
| 01 -- 05 | 1 | 1 | 1 |
| 06 -- 25 | 2 | 2 | 2 |
| 26 -- 50 | 3 | 3 | 3 |
| 51+ | 4 | 4 | 4 |
| Note: Code the Predominant severity level only | | | |

*3.1.2 Mix Design*

To match the mix design of the field sections, FDOT provided two aggregates and two asphalt binder types for the experiment which were combined with anti-strip and stability additives typical of PFC mixtures to create six mixtures for evaluation (summarized in Table 4). The aggregates provided were limestone and granite, and the asphalt binder provided was a PG 76-22 modified with either a polymer (PMA) or crumb rubber (ARB). These components will be discussed further subsequently.

**TABLE 4 Asphalt Mixture Descriptions**

| Mixture | Field Performance | Aggregate Type | Asphalt Type | OAC (%) | Anti-Strip (%) | Fiber[c] (%) |
|---|---|---|---|---|---|---|
| 1 | Good | Limestone + scrn | PG 76-22, PMA | 7.1 | 0.5[a] | 0.4 |
| 2 | Good | Limestone + scrn | PG 76-22, ARB | 7.1 | 0.5[a] | 0.4 |
| 3 | Poor | Limestone | PG 76-22, PMA | 6.1 | 0.5[a] | 0.4 |
| 4 | N/A | Limestone | PG 76-22, ARB | 6.1 | 0.5[a] | 0.4 |
| 5 | N/A | Granite | PG 76-22, PMA | 5.6 | 1.0[b] | 0.4 |
| 6 | N/A | Granite | PG 76-22, ARB | 5.6 | 1.0[b] | 0.4 |

[a] Liquid anti-strip was added at plant by weight of asphalt binder
[b] Hydrated lime was added to the aggregate in the laboratory by weight of aggregate
[c] Mineral fiber was added to the aggregate in the laboratory by weight of mixture

Three gradations were used to create 3 pairs of mixtures with the difference between asphalt mixtures within each pair being the type of asphalt binder used (PMA or ARB). As previously mentioned, asphalt mixtures 1, 2, and 3 match the mix design of the three field sections used as references to field performance. Mixture 4 is similar to mixture 3 except the ARB binder is used for mixture 4 instead of PMA. Mixtures 1 and 2 use the same limestone as mixtures 3 and 4, but mixtures 1 and 2 also incorporate limestone screenings producing a finer gradation. Mixtures 5 and 6 use a similar gradation to the coarser limestone mixtures with asphalt binder type, PMA or ARB, being the distinguishing factor. The mix design for mixtures 5 and 6 was evaluated since FDOT uses this mixture in the northern part of the state.

The OAC for all six mix designs was determined independently by FDOT using FM 5-588 (the pie-plate method) with PG 67-22 asphalt (*37*). As the asphalt binder contents of

these asphalt mixtures was high, which is typical of PFC, mineral fibers were added during mixing to prevent draindown. In addition, a liquid anti-strip agent (at 0.5% by weight of asphalt) was added to the asphalt binder at the plant for asphalt mixtures 1-4. Hydrated Lime was added at 1.0% by weight of aggregate during mixing to asphalt mixtures 5 and 6 as an anti-strip additive for the granite mixtures to match current FDOT mix design. Gradations for each mixture are shown in Table 5 and will be discussed in detail subsequently.

**TABLE 5 Aggregate Gradations for Asphalt Mixtures**

| Sieve Size | | Mixtures 1 & 2 | Mixtures 3 & 4 | Mixtures 5 & 6 |
|---|---|---|---|---|
| | | Limestone w/ Screenings | Limestone | Granite |
| 19.0mm | (3/4") | 100.0 | 100.0 | 100.0 |
| 12.5mm | (1/2") | 90.0 | 93.0 | 95.4 |
| 9.5mm | (3/8") | 66.0 | 69.0 | 72.6 |
| 4.75mm | (#4) | 24.0 | 23.0 | 19.8 |
| 2.36mm | (#8) | 10.0 | 9.0 | 9.0 |
| 1.18mm | (#16) | 8.0 | 5.0 | 6.6 |
| 600um | (#30) | 7.0 | 4.0 | 4.9 |
| 300um | (#50) | 6.0 | 3.0 | 3.9 |
| 150um | (#100) | 5.0 | 3.0 | 3.2 |
| 75um | (#200) | 3.5 | 3.0 | 2.8 |

### 3.2 Component Material Characterization

To understand the complex behavior of PFC asphalt mixtures, it is important to first understand the individual characteristics of its two main components, asphalt binder and

aggregate. Testing of the asphalt binder and aggregate consisted of standard and advanced tests as discussed in the following subsections.

### *3.2.1 Aggregate Analysis*

FDOT provided the basic physical properties of the aggregates including abrasion, polishing resistance, and water absorption based on their standard evaluation of the materials. These are summarized in Table 6. FDOT was not able to find all of the historical data on the testing and properties of the granite materials provided, so the summary only includes properties which had known or estimated values.

**TABLE 6 Aggregate Physical Properties**

| Aggregate Test | Limestone w/ Screenings | Limestone | Granite |
|---|---|---|---|
| Bulk Specific Gravity | 2.419 | 2.420 | ≈ 2.6[b] |
| Los Angeles Abrasion | 29.3 | 31.0 | N.A.[a] |
| Absorption | 2.77 | 2.64 | 0.78 |
| Insoluble Residue | 15.1 | 15.7 | N.A.[a] |

[a] Test data for Granite was not available from FDOT

[b] Not provided by FDOT but estimated from previous FDOT studies (*10; 32*)

Advanced testing (summarized in Table 7) was conducted as part of this study to investigate the morphological and thermodynamic properties of the granite and limestone. This information was used to characterize morphological properties of the aggregate and the quality of the bond between the aggregate and asphalt binder.

**TABLE 7 Aggregate Analysis**

| Aggregate Property | Test Method/Apparatus | Test Standard | Test Parameter |
|---|---|---|---|
| Form<br>Texture<br>Angularity | Aggregate Image Measurement System (AIMS) | AASHTO TP81 | Form, Texture, and Angularity Indices |
| Surface Free Energy (SFE) | Universal Sorption Device (USD) | Draft AASHTO Standard | SFE Components |

The Aggregate Image Measurement System (AIMS) was used to provide quantitative values for the aggregate morphological properties of angularity, form, and texture. Figure 7 provides an illustration of these properties. Angularity refers to variations at the corners of the aggregate, while form refers to variations in the shape of the particle. Texture refers to the surface texture of the aggregate at a microscopic level which does not affect the shape of the particle (*38*). These properties have been shown to impact the structural performance and skid resistance of asphalt mixtures (*39*).

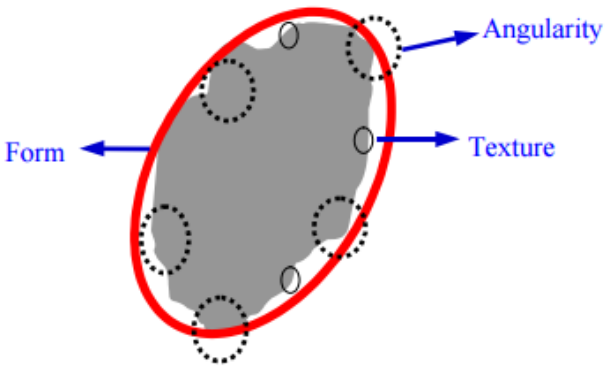


**FIGURE 7 Aggregate Shape Components: Angularity, Form, and Texture (*38*).**

The computer automated AIMS (Figure 8) utilizes image capture and analysis to characterize coarse and fine aggregate. It features top and back lighting, a high resolution camera, and a rotating circular tray system to collect and track individual aggregates. A single tray is loaded with particles from previously sieved, washed, and dried aggregate. Individual sieve sizes are analyzed one at a time. The aggregate is spaced to allow the camera to detect individual particles. The tray rotates and images are recorded and analyzed. The exact location of each particle is tracked to ensure that only particles that fall within the AIMS measurement specifications are included. The AIMS software then computes the values for the required morphological properties of each particle. The software provides an output of the distribution of values for each property as well as summary tables.

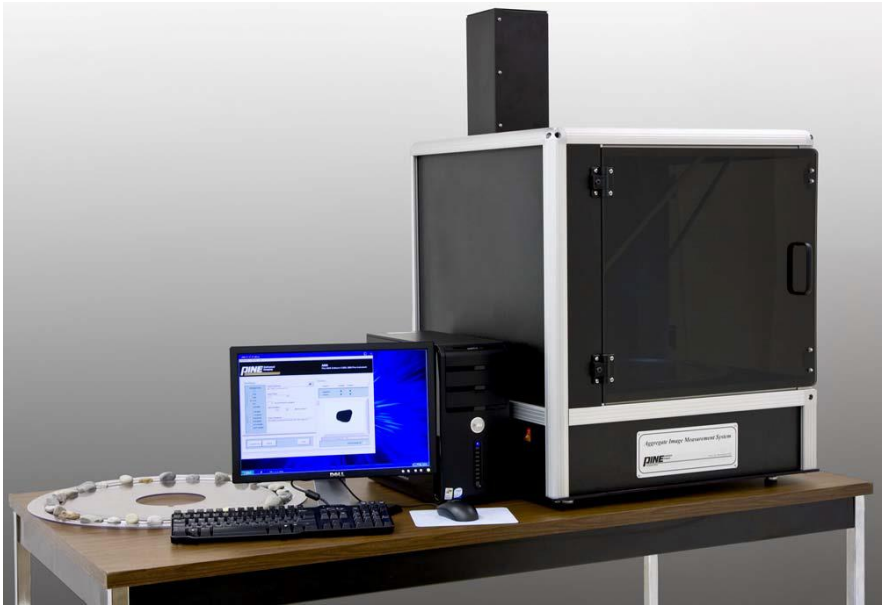

**FIGURE 8 Aggregate Image Measurement System (*39*).**

Various distresses in HMA pavements are caused by the failure of the adhesive bond between the aggregate and the asphalt binder. The SFE values of the component materials are used to calculate a quantitative measurement of the quality of that adhesive bond as well as its susceptibility to moisture interrupting the bond (*25*). This is important with respect to raveling as moisture susceptibility, specifically de-bonding between asphalt binder and aggregate, is a primary failure mechanism leading to raveling. The SFE components of each aggregate were determined by researchers at the University of Oklahoma using the Universal Sorption Device (USD). In the USD an aggregate sample is suspended in a chamber and a vacuum is applied. A probe vapor is released and allowed to adsorb onto the surface of the aggregate until a predetermined vapor pressure is reached. A magnetic balance measures the weight of probe vapor adsorbed. This is repeated at several predetermined vapor pressures. An isotherm is produced using the mass adsorbed relative to the vapor pressure for three different probe vapors from which the SFE components ($\gamma^{LW}$, the Lifshitz-van der Waals (LW) component; $\gamma^{+}$, the Lewis acid component; and $\gamma^{-}$, the Lewis base component) are determined.

### *3.2.2 Asphalt Binder Analysis*

FDOT provided two asphalt binders for testing. The first asphalt binder was a polymer-modified PG 76-22 asphalt binder (PMA), and the second asphalt binder was an Asphalt Rubber PG 76-22 asphalt binder (ARB). Both binders were provided in two conditions, neat (without any additives) and with a 0.5% (by weight of asphalt binder) liquid anti-strip agent which was added at the production plant. Table 8 summarizes the tests

executed to evaluate the asphalt binder. In addition, asphalt binder performance grading was conducted for verification according to AASHTO M320.

**TABLE 8 Asphalt Binder Analysis**

| Asphalt Property | Test Method/Apparatus | Test Standard | Test Parameter |
|---|---|---|---|
| Stiffness before and after Rolling Thin Film Oven (RTFO) and Pressure Aging Vessel (PAV) aging | Dynamic Shear Rheometer (DSR) | ASTM D7175 | G*/Phase Angle |
| Surface Free Energy (SFE) | Wilhelmy Plate (WP) | TTI Test Method | SFE Components |

To determine the response of each asphalt binder to aging, samples were run in the Dynamic Shear Rheometer (DSR) in unaged, short-term aged (after Rolling Thin Film Oven or RTFO), and long-term aged (after Pressure Aging Vessel or PAV) conditions. Two replicates were run for each test condition, and asphalt binder master curves were produced to determine asphalt binder susceptibility to aging.

SFE components of each asphalt binder type (PMA and ARB) at each condition (unaged, RTFO, PAV, Limestone Mastic, Granite Mastic) were determined using the Wilhelmy Plate (Figure 9). A dynamic contact angle (DCA) analyzer manufactured by Cahn was used to measure the contact angles of each asphalt binder under dynamic conditions. This device indirectly measures the contact angle between a glass slide coated with asphalt and a known liquid into which the slide is submersed. The contact angle is calculated using a relationship between the weight of the slide in air and as its

weight as it is being submerged, the known surface energy of the liquid, and the geometry of the slide. Average contact angles for each asphalt binder and condition in five different liquids were used to determine the three components of SFE ($\gamma^{LW}$, $\gamma^{+}$, and $\gamma^{-}$) for each asphalt binder testing condition. The liquids used for this experiment were distilled water, glycerol, ethylene glycol, formamide, and diiodomethane.

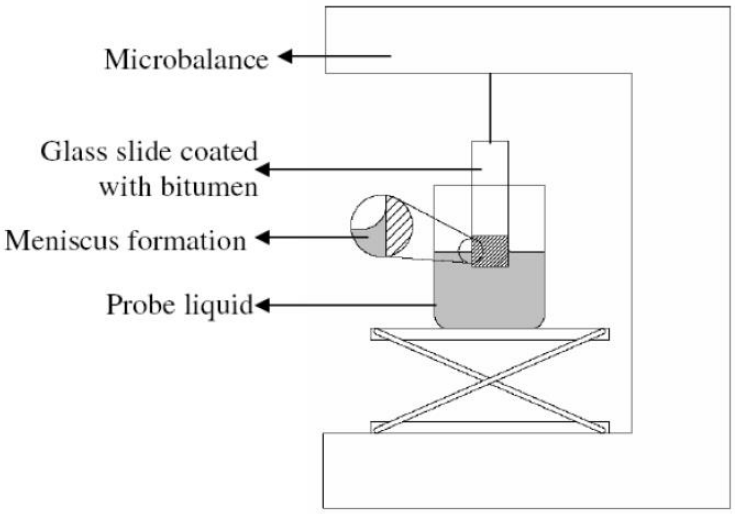


**FIGURE 9 Test Setup for Wilhelmy Plate (*26*).**

### 3.3 Asphalt Mixture Characterization

As the goal of this research is to correlate the laboratory performance of moisture conditioned, laboratory compacted specimens to the performance of asphalt mixtures in the field; specimens had to be prepared to replicate the in-place field sections. This required careful control of gradation, volumetrics, and specimen fabrication protocols. Finally, moisture conditioning and a robust testing protocol to accurately capture the

response of the asphalt mixtures was required. Table 9 summarizes the testing protocol utilized for each asphalt mixture.

**TABLE 9 Asphalt Mixture Analysis**

| Mixture Test | Test Method/Apparatus | Test Standard | Test Parameter | Specimen Height |
|---|---|---|---|---|
| Air Voids | Dimensional Analysis | ASTM D3203 | Total Percent Air Voids | All samples |
| Falling Head Permeameter | Permeability | Florida FM 5-565 | Coefficient of Permeability | 115mm |
| Cantabro Loss | LA Abrasion w/o Spheres* | AASHTO TP108 | Percent loss of material with and without moisture conditioning | 115mm |
| Indirect Tensile Strength (IDT) | Indirect Tensile Strength* | ASTM D6931 | IDT Strength and Tensile Strength Ration (TSR) | 75mm |
| Rutting and Stripping | Hamburg Wheel Tracking Test (HWTT) | AASHTO T324 | Rut depth with load cycles and load cycles to stripping number | 62mm |

*Before & After Moisture Induced Sensitivity Test (MIST)

### *3.3.1 Gradation*

The first step in producing the asphalt mixtures was ensuring the proper gradation of aggregates. Figure 10 shows the gradations for the three asphalt mixture pairs plotted against the 0.45 power curve. Aggregates were provided by FDOT in 5-gallon buckets from aggregate stockpiles. Originally, FDOT recommended batching aggregate from each stockpile at prescribed percentages, but it was quickly discovered that the actual gradation of the aggregate provided did not match the historically required batch percentages. In addition, the aggregate was noticeably wet and muddy. Therefore, all aggregate received from FDOT was oven dried at 110°C for 24 hours then allowed to cool and finally sieved and separated into individual sieve sizes. Each separated aggregate was then stored for the duration of the project in separate 5-gallon buckets (i.e.

buckets with all aggregate passing 4.75 mm (no. 4) sieve and retained on 2.36 mm (no. 8) sieve and batched as required for each mixture.

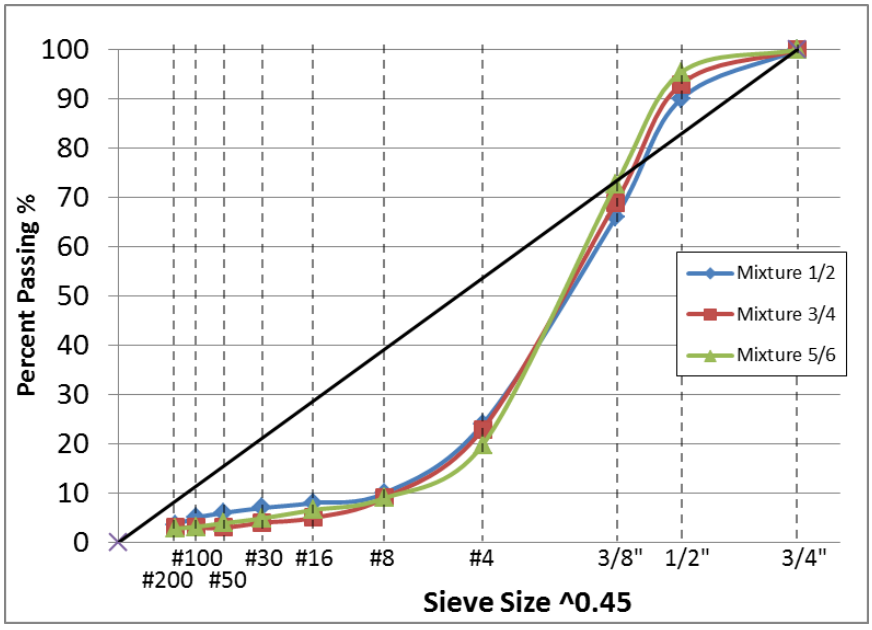


**FIGURE 10 Aggregate Gradations.**

Wet sieve analysis was conducted according to ASTM C117 to account for fines in the aggregates. Two 2500g samples were batched to meet the required gradation. Both samples were covered with water and agitated to bring the fines into suspension. The rinse water was poured over a pair of nested sieves (1.18 mmm (no. 16) sieve on top and 75 µm (no. 200) sieve on bottom). This rinse process was repeated until the agitated water was clear indicating most of the fines had been rinsed from the aggregate and the portion larger than 75 µm (no. 200) sieve had been collected on that sieve. The remaining material from the bowl and the material retained on the two sieves was

combined and dried to determine the percent of material passing the 75 μm (no. 200) sieve.

The iterative process of wet sieve analysis was continued until the differences between the target gradation, required by FDOT, and the gradation after wet sieve analysis fell to 1 percent for particle sizes larger than 4.75 mm (no. 4) sieve and 0.5 percent for particles between 4.75 mm (no. 4) sieve and 0.15 mm (no. 200) sieve. Table 10 shows the final results of the wet sieve analysis compared with the target gradations. The washed gradations were then used to batch all asphalt mixtures for testing.

**TABLE 10 Final Gradation Results of Washed Sieve Analysis**

| Sieve Size | | Mixtures 1 & 2 | | Mixtures 3 & 4 | | Mixtures 5 & 6 | |
|---|---|---|---|---|---|---|---|
| | | Original | Washed | Original | Washed | Granite | Granite |
| 19.0mm | (3/4") | 100.0 | **100.0** | 100.0 | **100.0** | 100.0 | **100.0** |
| 12.5mm | (1/2") | 90.0 | **88.8** | 95.4 | **92.7** | 95.4 | **95.2** |
| 9.5mm | (3/8") | 66.0 | **64.0** | 72.6 | **69.4** | 72.6 | **72.9** |
| 4.75mm | (#4) | 24.0 | **19.0** | 19.8 | **22.0** | 19.8 | **16.8** |
| 2.36mm | (#8) | 10.0 | **5.6** | 9.0 | **8.7** | 9.0 | **8.7** |
| 1.18mm | (#16) | 8.0 | **4.4** | 6.6 | **4.7** | 6.6 | **6.4** |
| 600um | (#30) | 7.0 | **4.2** | 4.9 | **3.6** | 4.9 | **4.6** |
| 300um | (#50) | 6.0 | **4.2** | 3.9 | **2.5** | 3.9 | **3.7** |
| 150um | (#100) | 5.0 | **4.2** | 3.2 | **2.5** | 3.2 | **2.9** |
| 75um | (#200) | 3.5 | **2.8** | 2.8 | **2.5** | 2.8 | **2.5** |

*3.3.2 Volumetrics and Specimen Fabrication*

Having determined the appropriate aggregate gradation from washed sieve analysis and given the OAC for each mixture from FDOT, the mixture components were ready to be combined. First, theoretical maximum specific gravity, $G_{mm}$, was first determined for all asphalt mixtures. Previous experience with PFC mixtures suggested the high OAC and particularly sticky nature of modified binders would prohibit using ASTM D2041 to determine $G_{mm}$ (*40*). It was suggested that reproducible results could not be achieved due to the inability to sufficiently separate particles and a loss of asphalt binder from excessive draindown. A trial batch was produced, and it was determined that draindown was not an issue for these mixtures (likely due to the addition of mineral fiber) and that with particular care and effort mixture clumps could be separated sufficiently. Therefore, the procedure outlined in ASTM D2041 was used to determine $G_{mm}$ for each asphalt mixture at the OAC provided by FDOT. Initially two 2500 gram replicates were used to determine $G_{mm}$ for each asphalt mixture but additional replicates were eventually run for asphalt mixtures 2, 5, and 6 to confirm the results.

The target air voids content for all LMLC specimens was 20% ±2%. The bulk specific gravity, $G_{mb,}$ and the air voids content for each compacted sample was determined by dimensional analysis as recommended by Alvarez et al (*40*). Equation 10 was used to calculate $G_{mb}$.

$$G_{mb-dimensional} = \frac{\frac{W}{V_{tot}}}{\rho_w} \quad (10)$$

Where:

$W$ = weight of the specimen in air, g

$V_{tot}$ = volume of the specimen, $cm^3$

$\rho_w$ = density of water, $g/cm^3$

The volume of each specimen was measured with the following process. The average height was determined from four height measurements taken with digital calipers at quarter intervals around the circumference of the specimen. The average diameter was also determined with digital calipers using two top-diameter measurements and two bottom-diameter measurements. The volume of the compacted specimen was considered to be a cylinder and calculated using Equation 11.

$$V_{tot} = \frac{\pi \cdot d^2 \cdot h}{4} \quad (11)$$

Where:

d = average measured diameter of specimen, cm

h = average measured height of the specimen, cm

$G_{mm}$ and $G_{mb\text{-}dimensional}$ were then used to estimate the volumetric properties of each compacted specimen with Equation 12 being utilized to calculate air voids.

$$\text{Total AV content} = 100 \times \left(1 - \frac{G_{mb}}{G_{mm}}\right) \ (\%) \quad (12)$$

Given the previously determined $G_{mm}$ for each mixture and knowing that dimensional analysis was required to calculate air voids, it was necessary to compact specimens to a specific $G_{mb}$ to achieve target air voids. This value was based on the weight of asphalt mixture placed in the mold, the diameter of the mold, and the final height of compaction. However, as previous research (*40*) and laboratory experience had noted; compacted PFC specimens tend to expand in the vertical direction after extraction from the SGC. In addition, the loose asphalt mixture structure can cause some PFC specimens to fall apart if not confined after extraction. To prevent the compacted specimens from falling apart, all compacted specimens were extracted into, and subsequently cooled overnight in, a 6-inch PVC pipe used as a mold. The PVC mold was removed after the specimen cooled for 24 hours.

To determine a repeatable specimen fabrication protocol, multiple test specimens were compacted and measured. It was determined that compacted specimens grew more than 1.0mm depending on final height. Smaller specimens (<80mm) grew more than larger specimens (115mm). It was also found that although the SGC mold is 150mm, the extracted specimen diameter averaged 150.6mm. Therefore, when calculating the weight of asphalt mixture to place in the mold to achieve 20% air voids, each specimen was

assumed to have a diameter of 150.6mm, and the compaction height input into the SGC was 1.0mm to 1.5mm below the target height to allow for vertical expansion.

Compacted specimens were prepared for testing using AASHTO R30. A mixture and compaction temperature of 160°C (320°F) was prescribed by FDOT. Aggregates were batched according to the required mix design and dried at mixing temperature overnight. When hydrated lime was used for asphalt mixtures 5 and 6, it was added to the aggregate during batching and dried overnight. After drying, and before adding asphalt binder to the aggregates, mineral fiber was added at 0.4% by weight of mixture. Before compaction, the asphalt mixture was Short Term Oven Aged (STOA) at 160°C (320°F). To prevent over-aging when multiple asphalt mixture types were prepared on the same day, mixing and STOA times were staggered to allow for the compaction of one mixture while the other mixture was aging. This was especially necessary when compacting asphalt mixtures 5 and 6 due to the time needed to achieve the high number of gyrations required for those asphalt mixtures.

The SGC was used to compact all specimens at a compaction angle of 1.25° and a compaction pressure of 600 kPa. As previously discussed, compacted specimens were extruded directly into 6-inch PVC molds for cooling. The PVC molds were completely cut along one side to allow them to be expanded to accept the compacted specimen. Once extruded, the mold was then closed and sealed with duct tape to contain the compacted specimen. It was noted while compacting the first asphalt mixture that it was

not possible to compact the specimens to the required height necessary for the HWTT test (62mm) and meet the desired air void content. Several iterations of adding more or less mixture at different compaction heights led to this conclusion. Thus for all mixtures, HWTT samples would be compacted to 75mm and then trimmed.

Asphalt mixtures 5 and 6 proved to be especially difficult to compact. Several specimens from asphalt mixtures 5 and 6 were prepared based on volumetric properties and allowed to compact to 300 – 500 gyrations. Despite the high number of gyrations, these specimens exceeded the require height by an average of 2.5mm and exceeded target air voids by 2%. Thus specimens were compacted 10mm taller than required and trimmed to meet test height requirements. Additionally, for asphalt mixture 5 and 6, a maximum of 250 gyrations was specified for compaction. Only 2 of 38 compacted specimens from asphalt mixtures 5 and 6 required less than the prescribed maximum number of gyrations.

There were several compacted specimens that required trimming either as prescribed for the permeability test or, as discussed above, to meet air voids. For the permeability test, FDOT FM 5-565 requires that the top and bottom of each compacted specimen be trimmed by the thickness equal to the NMAS (*41*). All compacted specimens requiring trimming were trimmed using a diamond-tipped saw blade with a water cooling system. Trimmed specimens were then rinsed to remove debris from the trimming process, air dried for 48-72 hours, and further dried using the CoreDry device to remove excess

moisture. Trimmed specimens were allowed to cool to testing temperatures at least overnight prior to additional testing.

In total, 114 compacted specimens were prepared for testing. Volumetrics were determined using dimensional analysis between 24-72 hours after specimen compaction. Samples that were not immediately subjected to performance testing after cooling to testing temperatures were stored in a 20°C room. All compacted specimens were tested within 2 to 3 weeks of fabrication. The results of specimen fabrication and air void calculations for each mixture are summarized in Table 11.

**TABLE 11 Fabrication Summary with Volumetric Properties**

| Mixture | Height | Test Prepared For | Total Replicates | $G_{mm}$ | Average | | |
|---|---|---|---|---|---|---|---|
| | | | | | $G_{mb}$ | Air Voids, % | Gyrations |
| 1 | 115mm | Cantabro Loss | 6 | 2.308 | 1.835 | 20.5 | 45 |
| | 77mm[a] | Permeability | 3 | | 1.835 | 20.5 | 25 |
| | 75mm | IDT | 6 | | 1.826 | 20.9 | 79 |
| | 62mm[b] | HWTT | 4 | | 1.839 | 20.3 | 52 |
| 2 | 115mm | Cantabro Loss | 6 | 2.296 | 1.837 | 20.0 | 32 |
| | 77mm[a] | Permeability | 3 | | 1.848 | 19.5 | 18 |
| | 75mm | IDT | 6 | | 1.823 | 20.6 | 95 |
| | 62mm[b] | HWTT | 4 | | 1.857 | 19.1 | 49 |
| 3 | 115mm | Cantabro Loss | 6 | 2.319 | 1.860 | 19.8 | 92 |
| | 90mm[a] | Permeability | 3 | | 1.848 | 20.3 | 41 |
| | 75mm | IDT | 6 | | 1.846 | 20.4 | 170 |
| | 62mm[b] | HWTT | 4 | | 1.874 | 19.2 | 170 |
| 4 | 115mm | Cantabro Loss | 6 | 2.342 | 1.871 | 20.1 | 78 |
| | 90mm[a] | Permeability | 3 | | 1.874 | 20.0 | 45 |
| | 75mm | IDT | 6 | | 1.860 | 20.6 | 167 |
| | 62mm[b] | HWTT | 4 | | 1.892 | 19.2 | 146 |
| 5 | 115mm | Cantabro Loss | 6 | 2.434 | 1.935 | 20.5 | 250[d] |
| | 90mm[a] | Permeability | 3 | | 1.979 | 18.7 | 245[d] |
| | 75mm[c] | IDT | 6 | | 1.918 | 21.2 | 250[d] |
| | 62mm[c] | HWTT | 4 | | 1.913 | 21.4 | 250[d] |
| 6 | 115mm | Cantabro Loss | 6 | 2.448 | 1.956 | 20.1 | 250[d] |
| | 90mm[a] | Permeability | 3 | | 1.983 | 19.0 | 283[d] |
| | 75mm[c] | IDT | 6 | | 1.946 | 20.5 | 250[d] |
| | 62mm[c] | HWTT | 4 | | 1.934 | 21.0 | 250[d] |

[a] Air voids for permeability specimens reflect height after trimming NMAS from top and bottom

[b] HWTT air voids reflect post-cut values

[c] All mixture 5 and 6 specimens were cut to achieve air voids

[d] Maximum gyrations was set to 250 for mixtures 5 and 6

*3.3.3 Laboratory Conditioning*

Laboratory moisture conditioning of LMLC specimens was conducted using the MIST device according to ASTM D7870 with deviations from the standard as noted in the following paragraph (*42*). Moisture conditioning in the MIST device subjects a specimen to higher than normal temperatures while under pressure and exerts a cyclic pore pressure within the asphalt mixture structure by inflating and deflating a bladder. This enables the researcher to rapidly simulate the moisture damage that occurs under traffic loading at normal temperatures.

Figure 11 shows a schematic of the MIST device loaded with two specimens, as was typically the case in this experiment. Compacted specimens were placed inside the MIST chamber. Water was added to fill the chamber and submerge the compacted specimens. The top of the device was screwed on and water was added to an overflow device to ensure the chamber was completely filled. The device then heated and held the water at 60°C. The unit pressurized itself to 276 kPa using a bladder at the bottom of the chamber. When the set temperature and pressure were achieved, the device cycled the pressure 1000 times to condition the specimen. 1,000 cycles was used for this experiment as previous laboratory experience with PFC had shown that the 3,500 cycles recommended by ASTM D7870 caused many PFC samples to crumble. After MIST conditioning, specimens were then conditioned in a water bath at 25°C for one hour before being allowed to air dry for 48-72 hours. Excess moisture was then removed with the CoreDry device according to ASTM D7227.

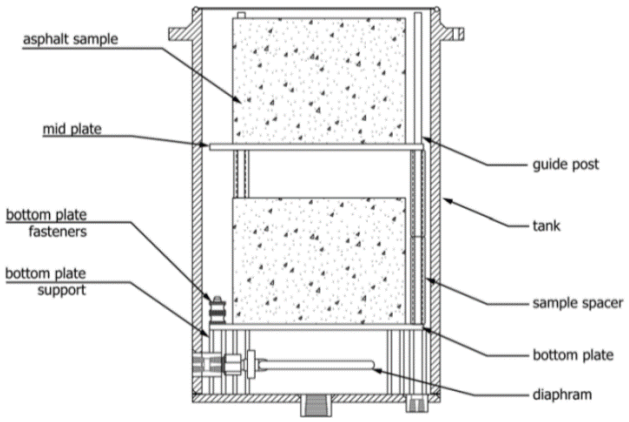


**FIGURE 11 MIST Test Setup with Two Specimens (*42*).**

To test each asphalt mixture's susceptibility to moisture damage, the IDT and Cantabro tests were run on specimens before and after laboratory conditioning with the MIST. The expectation was that as specimens were conditioned in the MIST to induce stripping, their post-MIST IDT and Cantabro results would be lower than those of the unconditioned specimens.

*3.3.4 Performance Testing*

Four tests were used to measure the performance characteristics of the asphalt mixtures. Three destructive tests and one non-destructive test were performed. The destructive tests were the IDT Strength Test, the Cantabro Loss, and the HWTT. The test for permeability was non-destructive.

Permeability was measured using the FDOT falling head permeameter test according to FM 5-565. In this test, saturated 6-inch diameter compacted specimens (tested in

triplicate) are placed inside an apparatus that seals around the sides of the specimen. A fixed amount of water (500ml) is then permitted to flow from a graduated cylinder through the specimen. The amount of time it takes (in seconds) for the water to flow through the specimen is recorded. The test is repeated until three times are recorded that fall within 4% of each other. The coefficient of permeability, k, is then calculated using Equation 13 and reported in whole units x $10^{-5}$ cm/s (*41*). For comparison with standard values in literature this number is converted to meters per day

$$k = \frac{aL}{At} \ln \frac{h_1}{h_2} \times t_c \quad (13)$$

Where:

a = inside cross-sectional area of the graduated cylinder, $cm^2$

L = average thickness of the test specimen, cm

A = average cross-sectional area of the test specimen, $cm^2$

t = elapsed time between $h_1$ and $h_2$, s

$h_1$ = initial head across the test specimen, cm

$h_2$ = final head across the test specimen, cm

$t_c$ = temperature correction for viscosity of water from 20°C standard

The Cantabro Loss test has been recommended by several researchers as one of the best tests to assess the durability of a PFC asphalt mixture (*2; 27; 28*). Provisional standard AASHTO TP108 was used to conduct this test where, one at a time, MIST conditioned

and unconditioned specimens were placed inside the LA Abrasion drum without the metal spheres. The specimen was allowed to freely rotate within the drum at a rate of 30-33 revolutions per minute for 300 revolutions. After 300 revolutions, the loose material was discarded and the ratio between the final weight and the initial weight was calculated. The ratio of the average MIST conditioned Cantabro Loss to the average unconditioned Cantabro Loss was also calculated. Three replicates were used per asphalt mixture per testing condition, and the test was performed at room temperature.

ASTM D6931 was used to measure the IDT of MIST conditioned and unconditioned specimens. Three replicates were used for each condition. The test consisted of a 75mm tall 6-inch diameter laboratory compacted specimen being compressed in the prescribed load frame at a rate of 2-in (50mm) per minute. The maximum load was recorded, and the IDT strength was calculated according to Equation 14. The ratio of the average MIST conditioned IDT strength to the average unconditioned IDT strength provides the TSR for the asphalt mixture. The test was performed at room temperature.

$$S_t = \frac{2000 \times P}{\pi \times t \times D} \quad (14)$$

Where:

$S_t$ = IDT strength, kPa

P = maximum load, N

t = specimen height immediately before test, mm

D = specimen diameter, mm

The final performance test was the HWTT, which was done in accordance with AASHTO T324. This test has been widely used to predict the moisture susceptibility and rutting resistance of asphalt mixtures, simultaneously. Two compacted specimens are placed in a 50°C water bath below a steel wheel. There are two wheels per test apparatus, so four specimens can be tested at once producing two test replicates. The wheels are lowered and the specimens are allowed to condition for 30 minutes in the water bath. The wheels are then rolled over the paired specimens at a rate of 52 passes per minute until 20,000 passes are reached or the rut depth exceeds 0.5 inches (12.5mm).

Figure 12 shows the three stages a specimen typically experiences as it is loaded. The primary stage, known as the post-compaction or consolidation stage, occurs rapidly at the onset of loading. The secondary or creep phase may then continue for many load cycles depending on the asphalt mixture quality. The tertiary phase is the phase where the asphalt mixture is experiencing damage due to stripping.

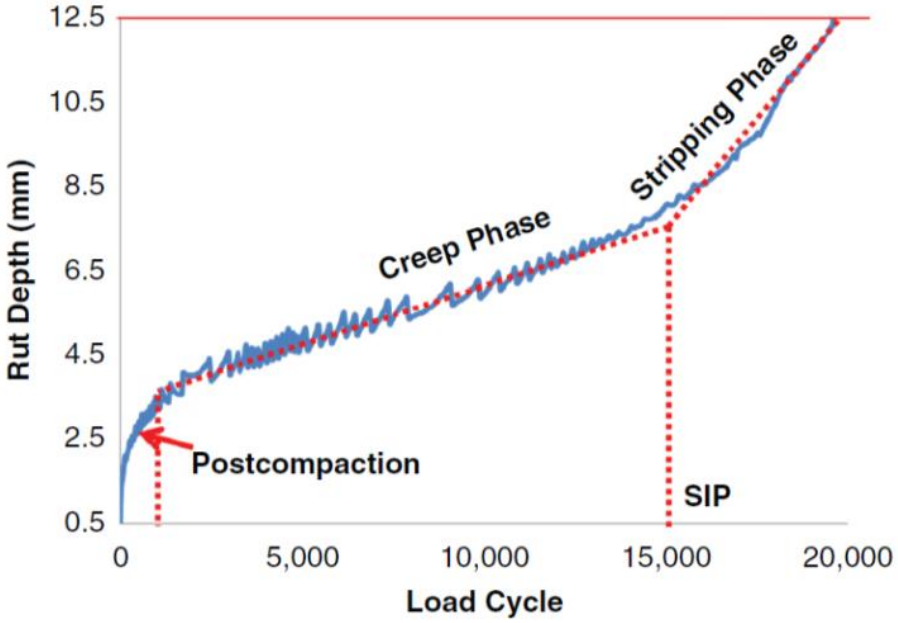


**FIGURE 12 Typical HWTT Output of Rut Depth vs. Load Cycle (*43*).**

In addition to the traditional output of rut depth versus load cycle, a novel analysis method developed by Yin et al. (*43*) was utilized. A curve is fit to the HWTT data and the inflection point of the curve is defined where the negative curvature of the creep phase changes to a positive curvature during the stripping phase. Illustrated in Figure 13, this point is labeled the stripping number (SN) and the number of load cycles at which the SN occurs ($LC_{SN}$) indicates the number of load cycles at which the material begins to soften because of the infiltration of water between the asphalt binder and aggregate. A lower $LC_{SN}$ represents an asphalt mixture that is more prone to stripping and thus is more susceptible to moisture damage (*43*).

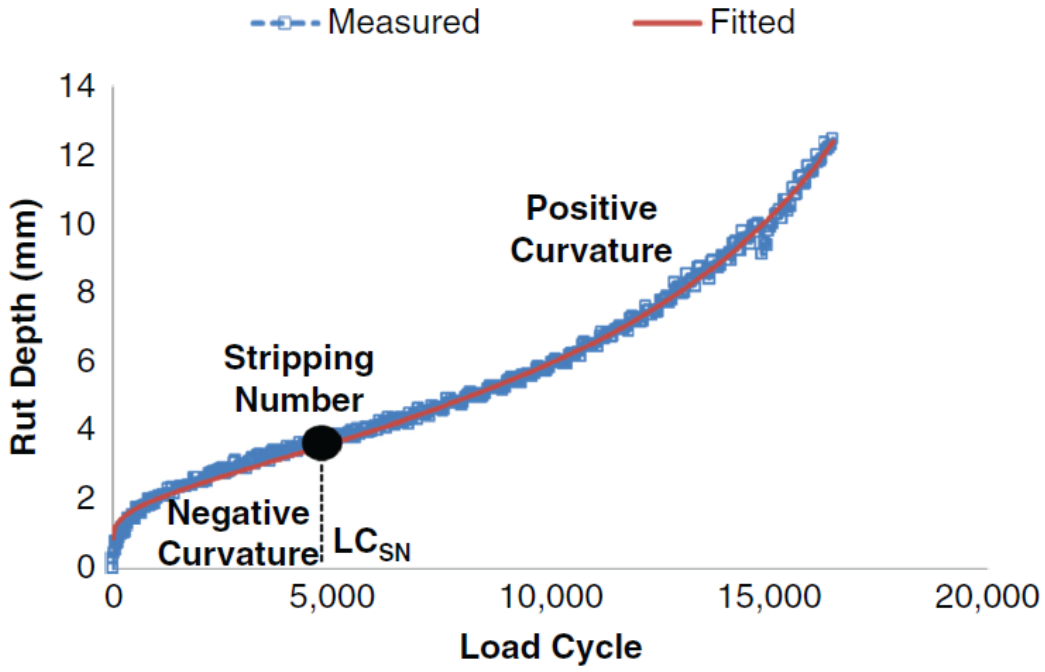


**FIGURE 13 Illustration of Novel HWTT Parameters (*43*).**

# 4. RESULTS AND ANALYSIS

This section provides the results of component material testing as well as the results of performance tests conducted on compacted specimens for all six asphalt mixtures, which were previously described in Table 4. The results of material testing are analyzed by component. Performance test results are presented and analyzed to determine which tests best correlate the moisture susceptibility of laboratory conditioned specimens with the field performance of asphalt mixtures 1-3 (see Table 4). Additional analysis as to which variables most influenced mixture performance is also provided.

## 4.1 Component Material Properties

Aggregates and asphalt binder used in the mix design for the selected asphalt mixtures were tested to determine the morphological, physical, and thermodynamic properties of the individual components as well as aggregate-asphalt binder combinations. AIMS analysis parameters and asphalt binder master curve data were used to characterize aggregates and asphalt binder, respectively. The SFE of each aggregate and asphalt binder was used to characterize the bond between the two materials for different aggregate-asphalt binder combinations at different asphalt binder aging states.

### *4.1.1 AIMS Parameters*

Aggregate analysis was conducted using the AIMS for the limestone and granite aggregates. Given the open-graded nature of the PFC mixture and the fact that the AIMS

is only capable of providing texture and sphericity index values for coarse aggregates (4.75mm (no. 4) sieve and above); results for angularity, texture, and sphericity were only attained for the coarse portion of each aggregate.

Prior to testing, each aggregate was separated into individual particle size groups by sieving. The sieves used for the coarse aggregates were the 19.0 mm (1/2”), 12.5mm (3/8”), and 4.75 mm (no. 4). Once separated, the sieved aggregates were washed over the 2.36mm (no. 8) sieve to remove surface dust and dried overnight in a 110°C oven. After cooling, individual particle size groups were placed in ziplock bags and stored at room temperature for later testing. Testing was conducted for both aggregates over a single day. The AIMS analyzed 50 particles from each particle size group and output a single value for angularity, texture, and sphericity based on the average value for each parameter across the 50 particles analyzed for the group. The angularity, texture, and sphericity values for each individual particle size were then combined into a single value for each aggregate. This was accomplished using Equation 15 by weighting the parameter value at each particle size based on the individual percent retained for the particle size as a portion of the total coarse aggregate gradation. The total course aggregate percent retained is the sum of the individual percent retained for the coarse portion of the total gradation (greater than 4.75mm (no. 4) sieve).

$$\frac{\sum(\%\ \mathrm{Ret.}_i \times \mathrm{Angularity}_i/\mathrm{Texture}_i/\mathrm{Sphericity}_i)}{\sum \%\ \mathrm{Retained}_{\mathrm{Coarse\ Agg.}}} \tag{15}$$

The final weighted averages for the three parameters for each aggregate are shown in Table 12.

**TABLE 12 AIMS Component Values**

| Aggregate | Angularity[a] | Texture[a] | Sphericity[a] |
|---|---|---|---|
| Limestone w/ Screenings | 2915.5 | 146.6 | 0.73 |
| Limestone | 2900.2 | 142.7 | 0.73 |
| **Limestone (Average)** | **2907.8** | **144.6** | **0.73** |
| **Granite** | **3047.2** | **227.6** | **0.67** |

[a] Average value weighted by coarse gradation only

The values for the two limestone gradations were averaged to create a single composite value for angularity, texture, and sphericity for limestone. The AIMS classification scale divides each parameter into low, moderate, high, and extreme ranges. This scale and the average parameter values from the AIMS results for limestone and granite are shown in Figure 14.

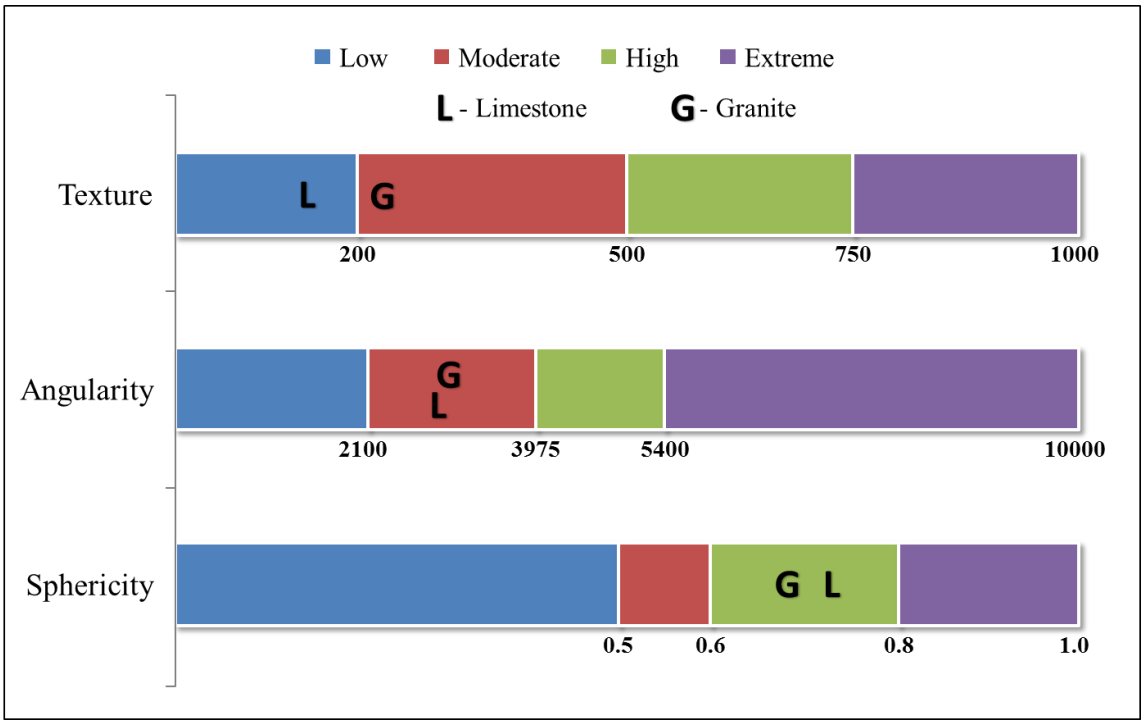


**FIGURE 14 Aggregate Texture, Angularity, and Sphericity Values.**

Based on Figure 14, it can be seen that the limestone aggregate has low texture, moderate angularity, and high sphericity. The granite aggregate has moderate texture (though on the low end of the range), moderate angularity, and high sphericity. A comparison of the aggregate texture, angularity, and sphericity for the two aggregates reveals limited differences between the limestone and granite for any parameter, though the higher texture value for granite may create a better interface for mechanical bonding between the aggregate and asphalt binder. However, the similarity of the results indicates that these morphological properties were likely not contributing factors to differences in moisture susceptibility and field performance between mixtures.

*4.1.2 Asphalt Binder Master Curves*

The two asphalt binder types, PMA and ARB, were tested using the DSR and ASTM 7175 with a modified frequency sweep method. The complex shear modulus, $G^*$, and phase angle, δ, were measured at different temperatures and frequencies of loading. Figure 15 provides an illustration of the testing methodology and factors used to collect and analyze the DSR data.

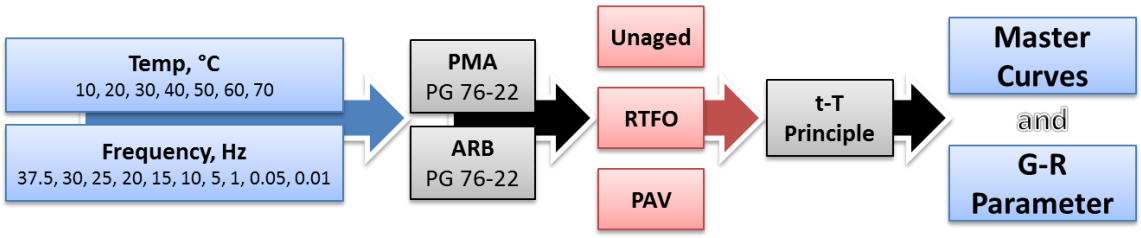


**FIGURE 15 DSR Data Collection and Analysis Methodology.**

Using the time-temperature (t-T) superposition principle, raw test data from the DSR was shifted to a reference temperature of 20°C using a t-T shift factor, $a_T$, applied to the frequency of loading. This t-T adjusted frequency is referred to as the reduced frequency. An extended CAM model (Equation 16) was used for the master curve, and the Williams-Landel-Ferry (WLF) model (Equation 17) was used for the t-T shift factor function (*44*).

$$|G^*| = G_g * \left(1 + \left(\frac{f_c}{f}\right)^k\right)^{-\frac{m_e}{k}} \quad (16)$$

Where:

$G_g$ = Maximum shear modulus or glass modulus, Pa

$f$ = Reduced frequency, Hz

$f_c$, $m_e$, k = fitting coefficients

$$\log a_T = \frac{C_1(T-T_R)}{C_2+T-T_R} \quad (17)$$

Where:

$T_R$ = Reference Temperature, °C – (20°C for this experiment)

$C_1$, $C_2$ = Fitting coefficients

After applying the t-T superposition principle to shift the test data for 10-70°C to the reference temperature (20°C), a single master curve was produced. The master curve describes the time dependency of the asphalt binder, while the amount of shift required to create a smooth function reflects the temperature dependency of the material. Master curves are made up of a large collection of shifted data points. To avoid cumbersome data display, they are best represented as a summary of their fitting parameters as shown in Table 13.

Master curves for both asphalt binders at multiple aging states are plotted in Figure 16, and the master curves for the unaged state of both binders are parallel across the full spectrum of loading temperatures and frequency with the PMA being slightly stiffer.

Aging appears to minimally affect both PMA and ARB at low temperatures or high frequency of loading. The effect of aging is more pronounced at high temperatures or low frequency of loading. Aging appears to affect the ARB more significantly at higher temperatures as the magnitude of the increase in complex shear modulus at intermediate and higher temperatures is greater for ARB than PMA from an unaged to RTFO state.

**TABLE 13 Master Curve Coefficients and G-R Parameters**

| | G* | | | $a_T$ | | G* | δ | G-R |
|---|---|---|---|---|---|---|---|---|
| | $f_c$ | $k$ | $m_e$ | $C_1$ | $C_2$ | @ $f$ = 0.005 rad/s | | Parameter |
| **PMA** | | | | | | | | |
| Unaged | 385.3 | 0.23 | 0.74 | -15.2 | 114.8 | 5.0E+04 | 85.5 | 307.2 |
| RTFO | 338.6 | 0.22 | 0.71 | -15.6 | 115.8 | 8.0E+04 | 84.8 | 646.2 |
| RTFO+PAV | 85.4 | 0.17 | 0.64 | -24.4 | 183.5 | 3.5E+05 | 79.1 | 12799.4 |
| **ARB** | | | | | | | | |
| Unaged | 659.3 | 0.20 | 0.75 | -13.7 | 104.8 | 2.8E+04 | 84.6 | 243.0 |
| RTFO | 102.8 | 0.17 | 0.75 | -15.6 | 112.2 | 8.4E+04 | 78.8 | 3263.3 |
| RTFO+PAV | 64.6 | 0.14 | 0.64 | -26.5 | 206.3 | 3.0E+05 | 74.7 | 21409.0 |

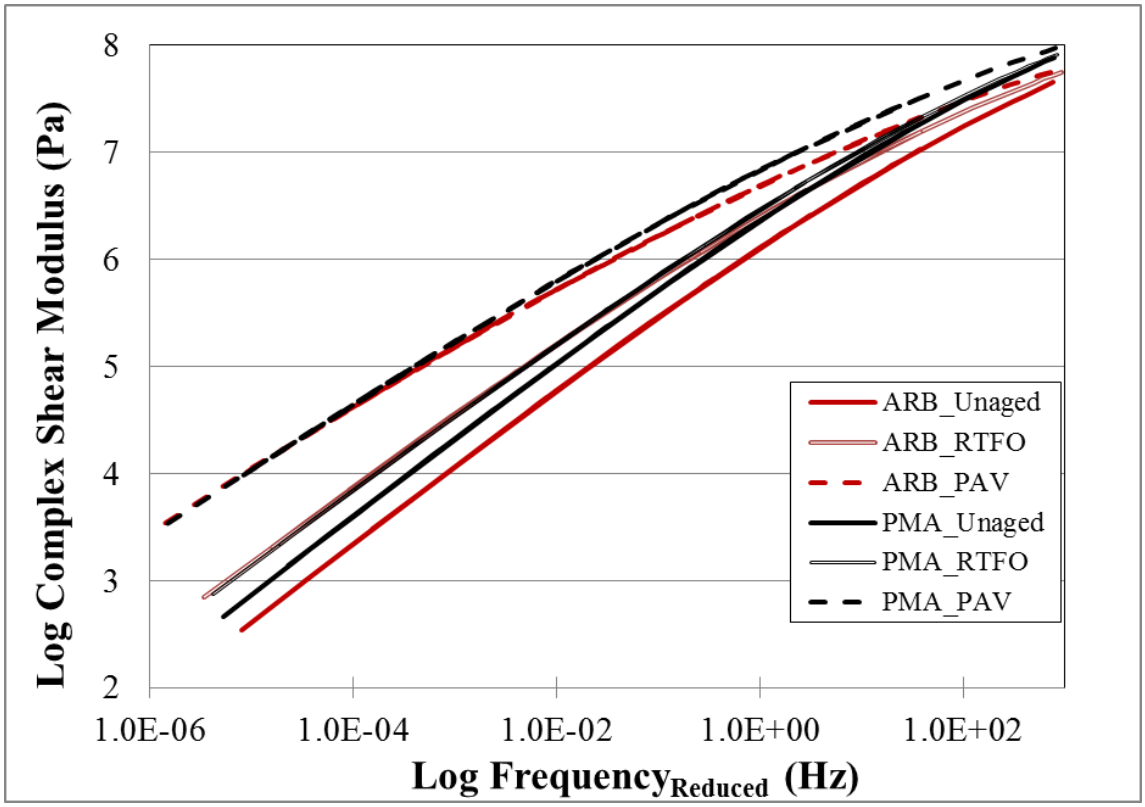


**FIGURE 16 Master Curves for PMA and ARB.**

To better quantify the expected impact of aging on the two asphalt binder types, an additional parameter was examined. Glover et al. (*45*) originally developed a single-point rheological parameter which provided a good predictor of asphalt binder resistance to failure due to oxidative hardening. Attained through DSR testing at 15°C and 0.005 rad/s, the parameter had excellent correlation with ductility and most importantly, it was found to be very reliable in predicting cracking performance with aging in the field. Rowe (*46*) modified the Glover parameter, and attained the form of the Glover-Rowe (G-R) parameter shown in Equation 18.

$$\text{G-R Parameter} = \frac{G^*(\cos\delta)^2}{\sin\delta} \quad (18)$$

In comparisons with cracking in the field it was shown that the onset of early raveling can be predicted with G-R parameter values ≥ 180 kPa and that significant cracking occurs with a G-R parameter value ≥ 450 kPa (*46*). This range of values for the G-R parameter, between 180 kPa and 450 kPa, is considered the damage zone for an asphalt binder.

The G-R parameter values for each binder type and aging state were included in Table 13 and plotted in Figure 17 on a Black Space plot. The Black Space plot shows G* and δ on a single graph which is useful to visualize the effect of aging on the rheological properties of the asphalt binder. The damage zone is also plotted on the Black Space plot representing the previously described G-R parameter threshholds of 180 kPa and 450 kPa. Asphalt binders that fall below this zone are not expected to experience cracking (*46*).

As asphalt binder ages, it becomes harder, less ductile and more prone to fracture. This behavior manifests as an increase in G* as the material becomes more stiff, and a decrease in δ as it becomes less viscous. DSR testing confirmed this expectation as the results plotted in Figure 17 show the G-R parameter value shifting up and to the left as the PMA and ARB asphalt binders age. From the G-R parameter plot, it is clear that neither asphalt binder is susceptible to failure due to oxidative hardening and that ARB

ages more rapidly than PMA. Indeed, a 1200% increase in the G-R parameter is seen in ARB after RTFO aging while PMA only experienced a 110% increase in the G-R parameter after the same short-term aging. This would indicate that the plant production process has a more damaging effect on ARB then PMA. From the PAV data points, the effect of long term aging is more pronounced in ARB than PMA. Overall it can be said that the ARB appears to be advancing faster to the onset of early raveling and cracking than the PMA.

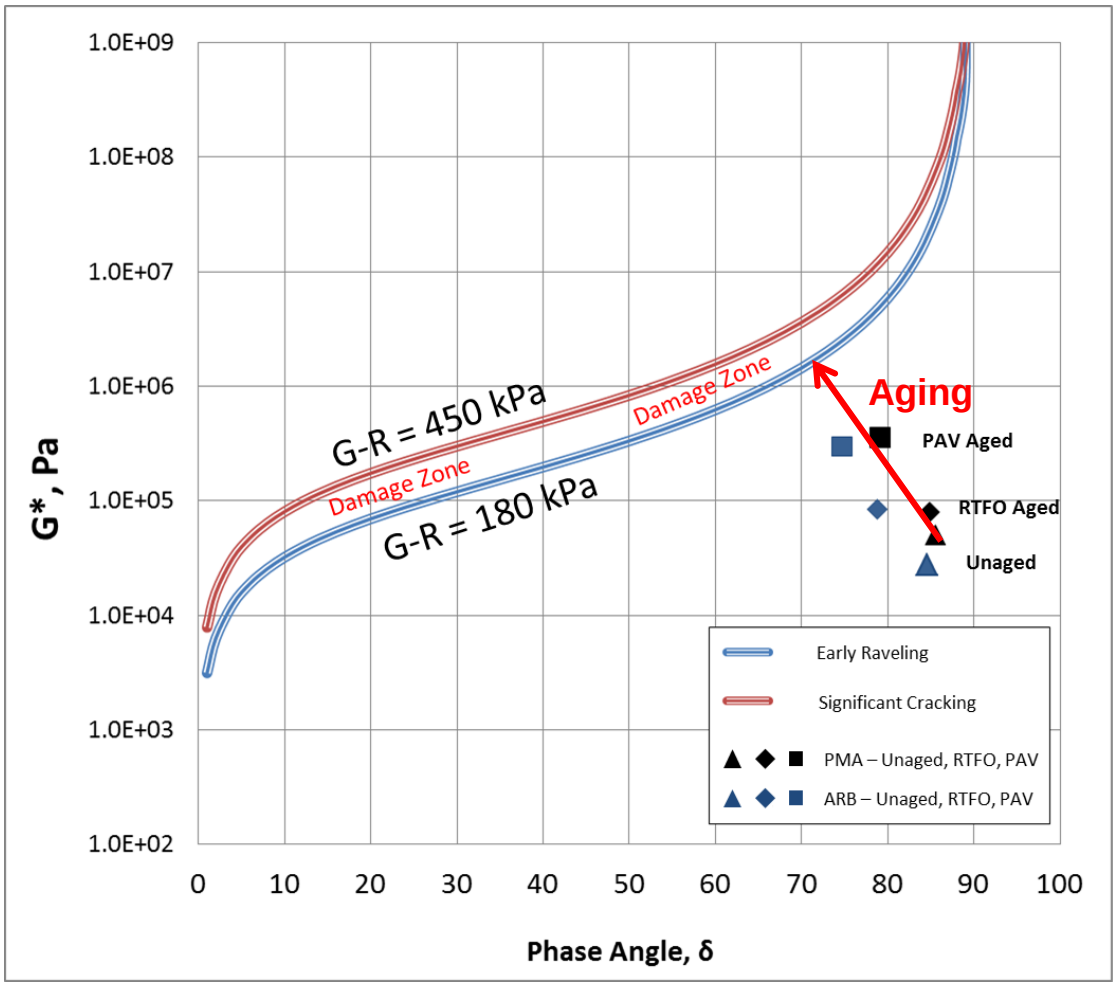


**FIGURE 17 Black Space Plot – G-R Parameters for PMA and ARB.**

*4.1.3 Surface Free Energy*

The SFE of the aggregates and the asphalt binder was measured to provide a means to characterize the strength of the adhesive bond between the aggregate and asphalt binder and the cohesive bond within the asphalt binder. The USD was used to determine SFE components for the limestone and granite, while the Wilhelmy Plate was used to determine SFE components for each asphalt binder at various states of aging. Equations 2 through 5 were then used to calculate the thermodynamic potential of the aggregate-asphalt binder combinations: $W_{\mathrm{AB}}$, the work of adhesion between the aggregate and the asphalt binder; $W_{\mathrm{ABW}}^{\mathrm{wet}}$, the work of debonding or the reduction of free energy when water displaces asphalt binder at the aggregate-asphalt binder interface; and $W_{\mathrm{BB}}$, the work of cohesion of the asphalt binder. Equations 6 through 9 were used to calculate the energy parameters: $ER_1$, $ER_2$, $ER_1$ * SSA, and $ER_2$* SSA.

As previously described in the experimental design, PMA and ARB were each tested in the following three aging states: unaged, RTFO, and PAV. The advancing and contact angles of asphalt binder coated slides were measured for all six asphalt binder states using the procedure outlined previously, and adapted from Little and Bhasin (*26*). This procedure required a number of trial batches to generate repeatable results. Particular care was given to producing asphalt covered slides of consistent thickness. This was found to reduce the variability of contact angle measurements between slides, requiring less slide replicates and improving the precision of the data. Once the contact angle data was acquired, the Young-Dupree equation (Equation 19) was used to calculate the SFE

components of each asphalt binder state. Equation 19 shows the relationship between the work of adhesion, $W_{LS}$ (from Equation 2); the measured contact angle, θ; and the SFE components of both the liquid (the various probe liquids) and the solid (asphalt binder) (*26*).

$$W_{LS} = \gamma_L(1 + \cos\theta) = 2\sqrt{\gamma_S{}^{LW}\gamma_L{}^{LW}} + 2\sqrt{\gamma_S{}^{+}\gamma_L{}^{-}} + 2\sqrt{\gamma_S{}^{-}\gamma_L{}^{+}} \quad (19)$$

In Equation 19, the total SFE ($\gamma_L$) and the three SFE components ($\gamma^{LW}$, $\gamma^+$, and $\gamma^-$) are known for the liquid from the literature, and the contact angle was measured using the Wilhelmy Plate. The three SFE components of the asphalt binder are unknown. By using contact angles from three probe liquids, a system of three equations with three unknowns can be solved for the unknown SFE components of the asphalt binder. The Little and Bhasin procedure (*26*) recommends the use of five probe liquids to improve the accuracy of the computed SFE components. The SFE components for the PMA and ARB asphalt binder at each aging state are summarized in Table 14.

The SFE components for limestone and granite were obtained using the USD, and are presented in Table 14 as well. The Branauer, Emmett, and Teller (BET) equation was used to estimate the specific surface area (SSA) of the aggregate from the adsorption isotherm for n-hexane (*26*). Due to laboratory equipment issues, the USD data set was obtained from researchers at the University of Oklahoma (OU).

**TABLE 14 Surface Energy Properties of Materials**

| | | Surface Energy Components (ergs/cm$^2$) | | | | Specific Surface Area (SSA) (m$^2$/gm) |
|---|---|---|---|---|---|---|
| | | $\gamma^{Total}$ | $\gamma^{LW}$ | $\gamma^{+}$ | $\gamma^{-}$ | |
| **Asphalt Binders** | | | | | | |
| PMA | Unaged | 16.42 | 12.53 | 0.44 | 8.61 | N/A |
| | RTFO | 12.16 | 7.48 | 2.64 | 2.08 | N/A |
| | PAV | 18.25 | 16.58 | 0.28 | 2.45 | N/A |
| ARB | Unaged | 22.21 | 22.21 | 0.00 | 3.43 | N/A |
| | RTFO | 21.90 | 21.90 | 0.00 | 5.29 | N/A |
| | PAV | 20.94 | 19.98 | 0.05 | 4.83 | N/A |
| **Aggregates** | | | | | | |
| Limestone | | 90.20 | 49.00 | 1.90 | 221.40 | 0.550 |
| Granite | | 515.20 | 51.90 | 86.70 | 619.30 | 0.354 |

N/A = Not Applicable

The value of total SFE for each asphalt binder ranges from 12.6 to 22.2 ergs/cm$^2$ which is at the low range of the typical results for asphalt binder (*26*). The LW component was the most significant contributor to the surface energy of the asphalt binders with a range from 7 to 22 ergs/cm$^2$. The Lewis acid component for all asphalt binders was very small ranging from 0.0 to 2.64 ergs/cm$^2$. The Lewis base component for all asphalt binders was small as well, ranging from 0 to 8.6 ergs/cm$^2$. The low Lewis acid and Lewis base values confirm the weak polar nature of asphalt binders (*26*).

Using this component SFE data, all possible combinations of aggregate and asphalt binder (with and without aging) were used to generate values for the thermodynamic potential of the aggregate-asphalt binder interface at different aging states in the presence of water. These values are provided graphically in Figure 18 to compare the work of adhesion, $W_{AB}$; work of debonding, $W_{ABW}^{wet}$; and work of cohesion, $W_{BB}$.

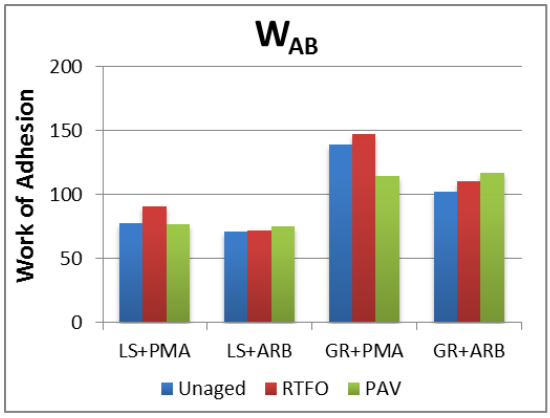


(a)

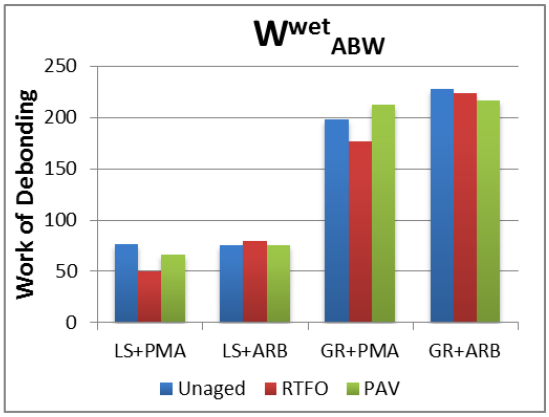


(b)

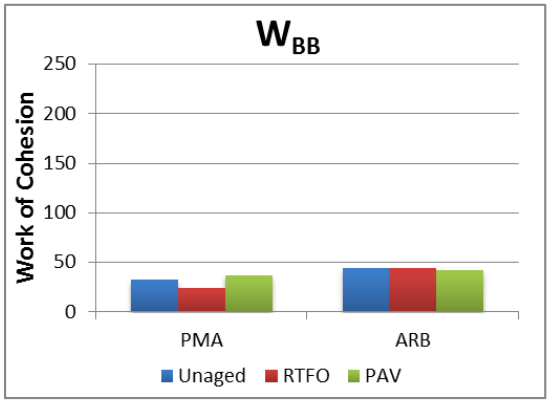


(c)

**FIGURE 18 (a), (b), (c) Thermodynamic Potential of Aggregate-Asphalt Binder Interface.**

For an aggregate to be durable and resistant to moisture damage, the work of adhesion between the aggregate and asphalt binder, $W_{AB}$, should be as high as possible. Similarly, the work of cohesion, $W_{BB}$, should be as high as possible to improve the durability of the asphalt binder. Also a higher magnitude of $W_{ABW}^{wet}$, the work of debonding, indicates a high thermodynamic potential for water to replace asphalt binder at the aggregate-asphalt binder interface, therefore it is desirable that this quantity be as small as possible to reduce moisture sensitivity. Figure 18(a) clearly shows that the granite-asphalt binder interface has a greater work of adhesion than the limestone-asphalt binder interface across all aging states. Thus it would be expected that it would take more work to displace asphalt binder from the granite surface than the limestone surface. Figure 18(b) shows that the average magnitude of the work of debonding at the granite-asphalt binder interface is much greater than at the limestone-asphalt binder interface. This would indicate that water has a greater attraction to the granite than it does the limestone which would indicate that it is more thermodynamically favorable to displace the asphalt binder from the granite than the limestone. Figure 18(c) indicates that the ARB has a slightly higher work of cohesion than the PMA indicating that the ARB may be more resistant to a loss of cohesion due to the presence of water.

The importance of the energy parameters is evident through examination of Figure 18. Results indicate that though there is better adhesion between the granite and asphalt binder in a dry environment, in the presence of water, there is a greater thermodynamic potential for debonding to occur at the granite-asphalt binder interface than the

limestone-asphalt binder interface. It would appear that the benefit of better adhesion may be countered by the preference of the system to replace asphalt binder with water. Therefore, it is important to consider the four energy parameters; $ER_1$, $ER_2$, $ER_1$ * SSA, and $ER_2$* SSA; to further evaluate mixture susceptibility to moisture damage. These values are summarized in Table 15.

**TABLE 15 Energy Parameters of Aggregate-Asphalt Binder Combinations**

| | $ER_1$ | $ER_2$ | $ER_1$ * SSA | $ER_2$ * SSA |
|---|---|---|---|---|
| **Limestone + PMA** | | | | |
| Unaged | 1.02 | 0.59 | 0.56 | 0.32 |
| RTFO | **1.82** | **1.33** | **1.00** | **0.73** |
| PAV | 1.17 | 0.62 | 0.64 | 0.34 |
| **Limestone + ARB** | | | | |
| Unaged | 0.94 | 0.36 | 0.52 | 0.20 |
| RTFO | 0.91 | 0.36 | 0.50 | 0.20 |
| PAV | 1.01 | 0.45 | 0.55 | 0.25 |
| **Granite + PMA** | | | | |
| Unaged | 0.70 | 0.54 | 0.25 | 0.19 |
| RTFO | 0.83 | 0.70 | 0.30 | 0.25 |
| PAV | 0.54 | 0.37 | 0.19 | 0.13 |
| **Granite + ARB** | | | | |
| Unaged | ***0.45*** | ***0.26*** | ***0.16*** | ***0.09*** |
| RTFO | 0.49 | 0.30 | 0.17 | 0.11 |
| PAV | 0.54 | 0.35 | 0.19 | 0.12 |
| **Highest Parameter Value** | | | | |
| ***Lowest Parameter Value*** | | | | |

The literature (*25; 26; 47*) is clear that the SSA of the aggregate has a significant impact on the correlation of the energy parameters to field performance. This is intuitive as the

work of adhesion or debonding occurs over the entire area of the aggregate, and a surface with high microtexture – a higher SSA – would have a greater surface over which to bond. Therefore, aggregate-asphalt binder combinations were ranked relative to each other by $ER_1$ * SSA, and $ER_2$* SSA as the asphalt binder aged. Higher values of the energy parameter are desired, with 1 being the highest rank and 4 being the lowest ranking. This analysis is summarized in Table 16.

**TABLE 16 Ranking of Aggregate-Asphalt Binder Moisture Susceptibility**

| | Unaged | | RTFO | | PAV | | Average |
|---|---|---|---|---|---|---|---|
| | $ER_1$*SSA | $ER_2$*SSA | $ER_1$*SSA | $ER_2$*SSA | $ER_1$*SSA | $ER_2$*SSA | Rank |
| Limestone + PMA | **1** | **1** | **1** | **1** | **1** | **1** | **1.0** |
| Limestone + ARB | 2 | 2 | 2 | 3 | 2 | 2 | 2.2 |
| Granite + PMA | 3 | 3 | 3 | 2 | 3 | 3 | 2.8 |
| Granite + ARB | 4 | 4 | 4 | 4 | 3 | 4 | 3.8 |

From analysis of this comparative approach, a combination of limestone and PMA produces the least moisture susceptible asphalt mixture while the granite and ARB combination produces the most moisture susceptible asphalt mixture. It is clear that limestone-asphalt binder combinations are less moisture susceptible than granite-asphalt binder combinations. In addition, aggregate-PMA combinations produce less moisture susceptible asphalt mixtures than aggregate-ARB asphalt mixtures. Finally, it is interesting to note that the moisture susceptibility rankings do not appear to be influenced by aging.

## 4.2 PFC Performance Tests

In order to achieve the stated research objective of recommending laboratory testing and conditioning protocols to best predict field performance of PFC mixtures, four laboratory performance tests were conducted. These tests included a permeability test, the HWTT, and two tests which included moisture conditioning as a performance factor: the IDT strength test and the Cantabro Loss test. Test results were analyzed for statistical significance and examined for a correlation to the field performance of mixtures 1-3, as shown in Table 4.

### *4.2.1 Permeability*

The permeability of LMLC specimens was tested using the FDOT falling head permeameter shown in Figure 19. Specimens were compacted to achieve the target air void content of 20±2%. As previously discussed, the different mixtures required a varying number of gyrations to achieve the target air voids, and the effect of the number of gyrations will be discussed subsequently. After compaction, specimens were trimmed by the asphalt mixture's NMAS as described previously. Three replicates were produced for each test, and average results are reported for each mixture.

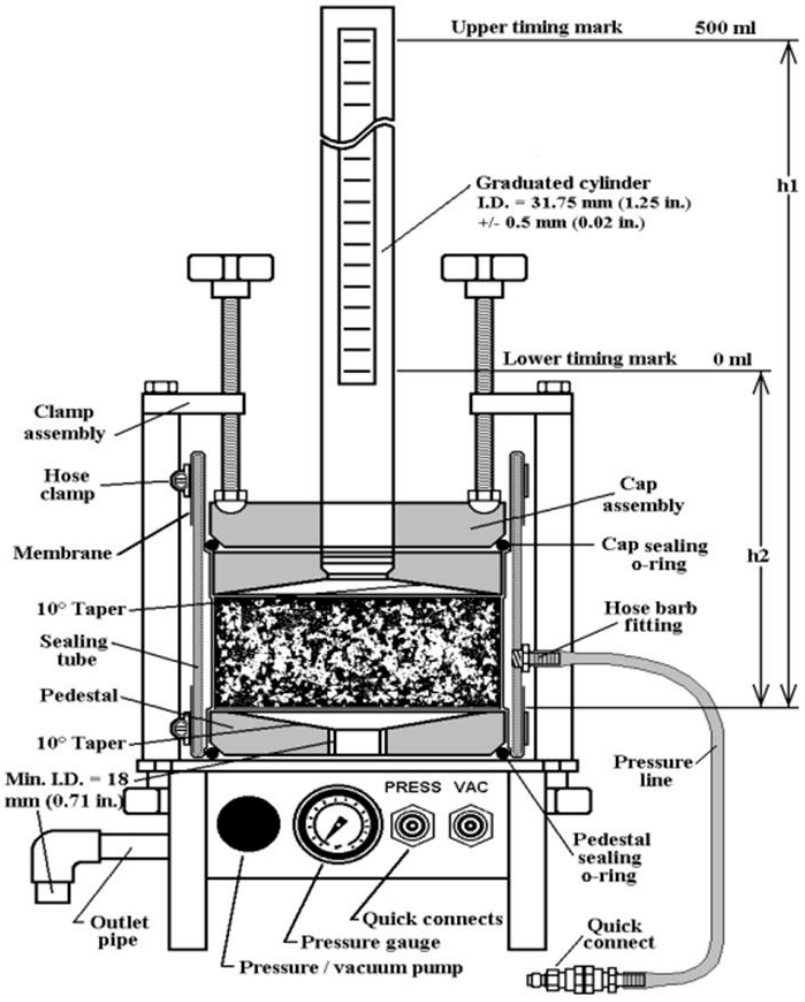


**FIGURE 19 FDOT Falling Head Permeameter (*41*).**

Prior to testing, specimens were allowed to saturate overnight in water. To ensure an adequate seal around the perimeter of the specimen, a layer of petroleum jelly was applied to the specimen perimeter. This application is shown in Figure 20. Once placed inside the permeameter, pressure was applied, at 69 kPa, to the rubber membrane surrounding the specimen and a water tight seal was achieved. This process ensures that

water is only traveling through the top and bottom of the specimen and not along the sides. To ensure the specimen remained saturated, water was continuously run through the specimen for 2 minutes ± 30 seconds.

**FIGURE 20 Permeability Specimen Ready to Test.**

The amount of time required for 500ml to flow through the specimen was recorded three times until the error between the first and third times was less than 4%. It was noted during testing that after the two minutes of additional saturation, there was never a problem achieving time differences less than 2%. It was also noted that for every specimen, the longer the test was run, the lower the recorded times were - but with no change in the error.

Previous research has recommended laboratory permeability values of 100 meters per day (*2*). For this study none of the asphalt mixtures met this requirement. The average value for each mixture is plotted in Figure 21. FDOT had provided guidance that the

permeability test was highly variable in PFC mixtures and test results confirmed this with a root mean square error (RMSE) of 7 meters per day.

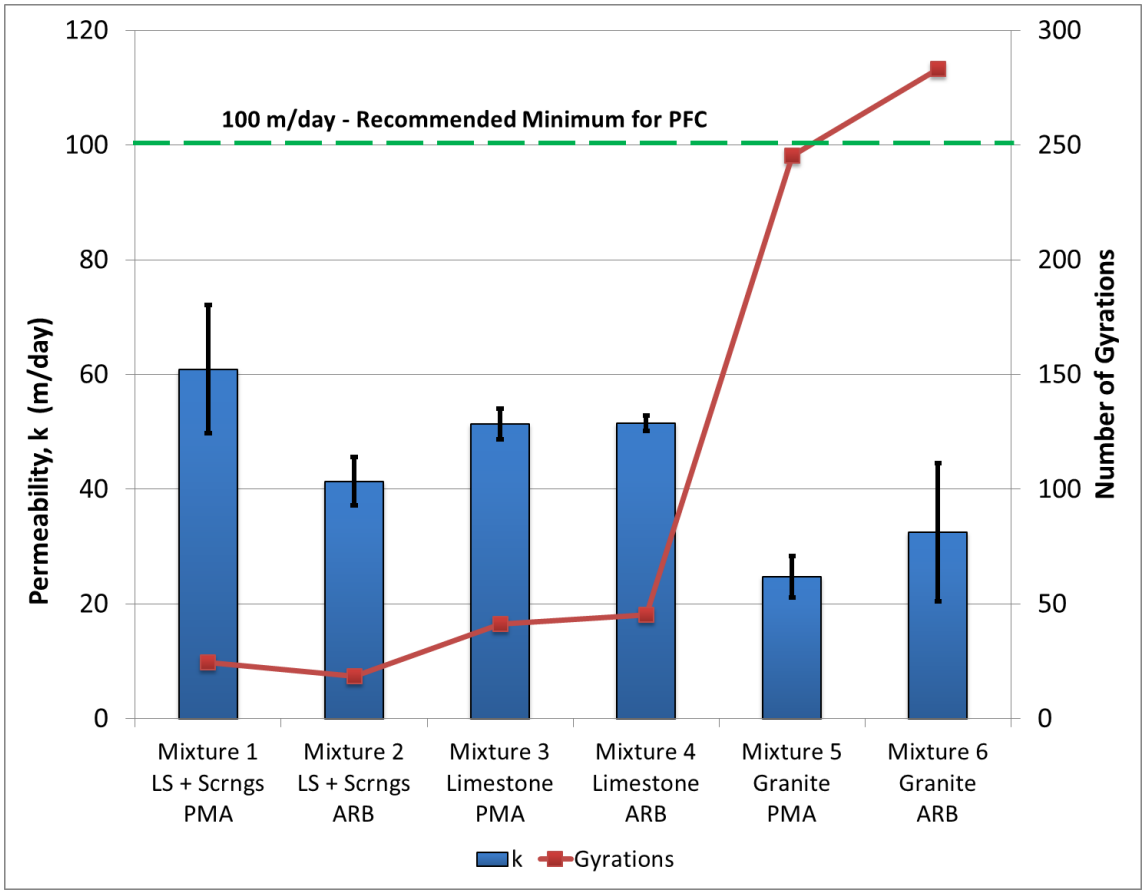


**FIGURE 21 Average Permeability with Number of Gyrations.**

Results show that mixture 1 was the most permeable and mixture 5 was the least permeable mixture. One-way Analysis of Variance (ANOVA) found that aggregate type, gradation, and gyration level all significantly affected permeability. It is important to note, however, that mixtures 5 and 6 required an average of 264 gyrations to meet the 20% air void requirement as opposed to the 32 gyration all other specimens required on

average. It is clear that the asphalt mixtures with the lowest permeability were the asphalt mixtures that were the most compacted. The higher compaction energy likely created smaller air voids and less interconnected air voids. At such a high compaction level, it is also likely that there may have been some aggregate fracture which would have changed the aggregate matrix inside the specimen. The combination of these factors most likely caused the decrease in permeability for mixtures 5 and 6. Due to the significant impact the number of gyrations had on test results, the controlling factor in the permeability tests was not a property of the asphalt mixture (gradation, binder, etc.), but an issue with specimen fabrication.

### *4.2.2 HWTT*

The HWTT was used to determine the moisture susceptibility and rutting resistance of the six asphalt mixtures. Four LMLC specimens were prepared for each asphalt mixture. Due to issues with achieving target air voids as previously discussed, specimens were compacted to 75mm and trimmed to 62±2mm. Specimens were then trimmed in accordance with AASHTO T324, cleaned of debris and tested in the HWTT. Since the HWTT test protocol has high temperature conditioning built in, no special conditioning provisions were applied. The test setup is shown in Figure 22.

**FIGURE 22 HWTT Setup.**

After the HWTT completed the 20,000 cycle program as specified previously and in AASHTO T324, maximum rut depth at the center point was recorded. None of the asphalt mixtures tested exceeded the maximum rut depth of 12.5mm. A disparity was noted between the maximum rut depth from the left and right wheels. The right wheel values were on average, two times greater than the left wheel average. As such, wheel location was used as a factor of interest in the regression analysis using least squares (LS) means.

A novel methodology created by Yin et al. (*43*) for analyzing the test data was originally proposed. Rut depth was plotted versus load cycles for all six asphalt mixtures, and it

was found that none of the plots reached the inflection point characteristic of SN, meaning that none of the asphalt mixtures experienced stripping and all had low moisture susceptibility. As none of the asphalt mixtures proved susceptible to stripping or rutting - according to the parameters of the HWTT – it was not possible to use the novel methodology. Therefore, conventional statistical analysis was used, and average maximum rut depths for both wheels are plotted in Figure 23.

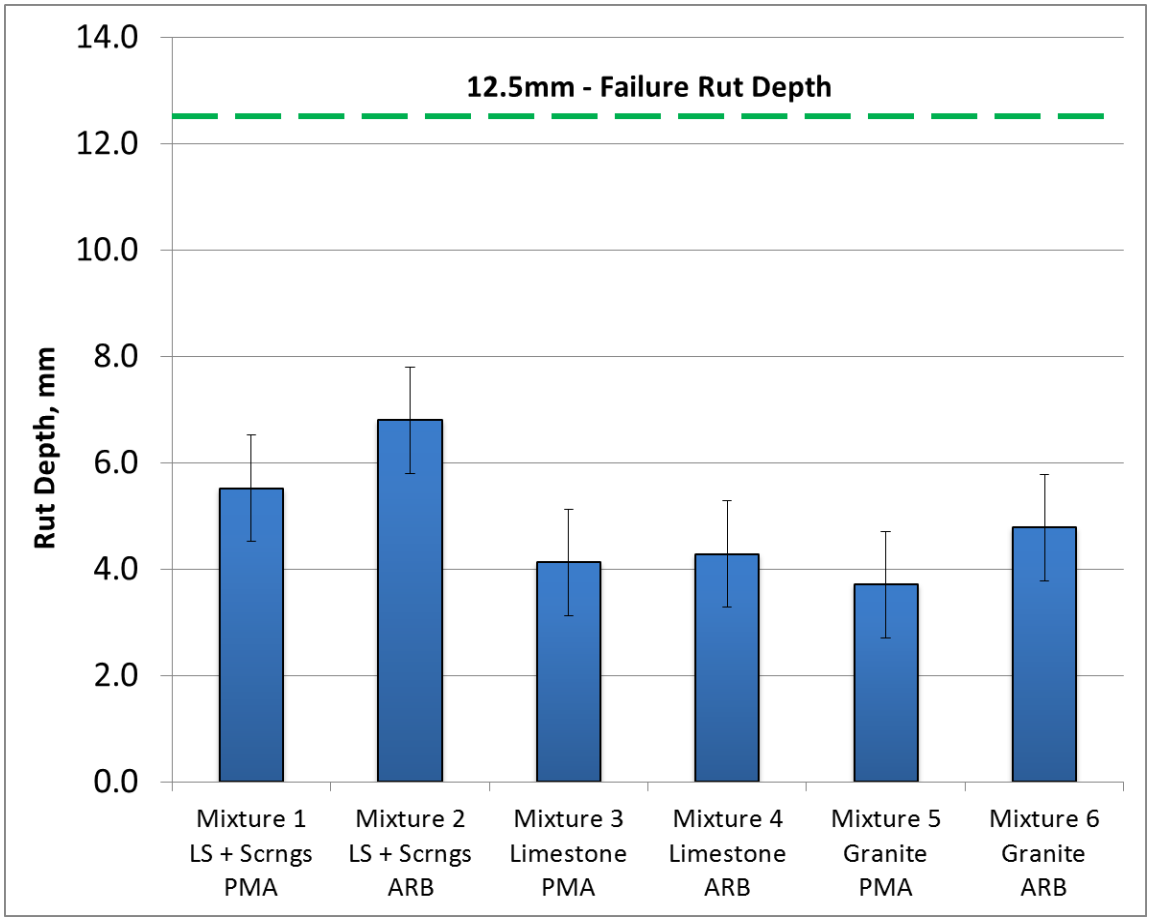


**FIGURE 23 Average Rut Depth by Asphalt Mixture.**

Results show that none of the mixtures failed due to rutting. The ANOVA model ($\alpha$ = 0.05) was fitted to the data with gradation, asphalt binder, and wheel as main effects and gradation/asphalt binder as a two-way effect. This analysis revealed that aggregate type and asphalt binder type did not influence rut depth. Further, it was determined that mixtures 1 and 2 were the most susceptible to permanent deformation while mixtures 3, 4, 5, and 6 were not different statistically.

### *4.2.3 IDT*

The IDT strength test was one of two tests used to measure the effect of the MIST laboratory moisture conditioning protocol on LMLC specimens. Three unconditioned (Pre-MIST) and three moisture-conditioned (Post-MIST) compacted specimens were tested in a load frame at a constant rate of 50mm per minute according to ASTM 6931. Tests were conducted at 20±2°C. Test results were recorded and the average values for each mixture were calculated along with the TSR, both of which are plotted in Figure 24.

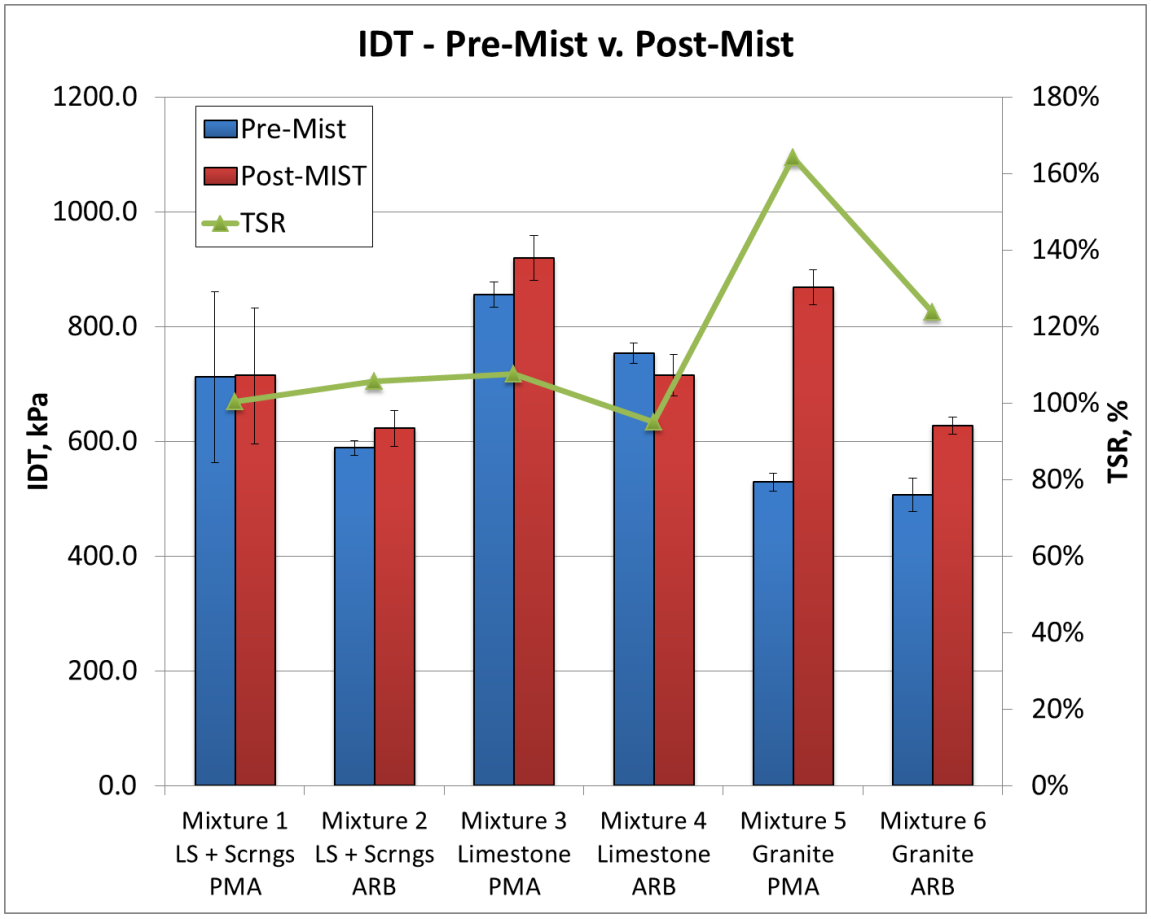


**FIGURE 24 IDT Strength and TSR Results.**

During testing the maximum load was achieved quickly (on average six seconds) and with very little deformation (3.5% average maximum strain). Figure 25 shows a specimen from mixture 6 after failure with 4% strain.

**FIGURE 25 Mixture 6 IDT Specimen Failure.**

RMSE for all 36 observations was 60kPa. In terms of IDT strength, analysis of the results revealed that mixture 3 had the highest average IDT strength while mixture 6 was the weakest mixture. Observational results show that for all mixtures except mixture 4, TSR was above 100% suggesting an increase in IDT strength with conditioning, which was opposite to the research hypothesis of decreasing IDT strength with conditioning. However, statistical analysis showed that conditioning was not statistically significant in all cases. Using the ANOVA model ($\alpha = 0.05$) with gradation, asphalt binder, and conditioning as main effects and all possible two-way effects between them considered, it was determined that while mixtures 5 and 6 were affected by conditioning, conditioning *did not* significantly affect IDT strength for mixtures 1-4. Therefore

mixtures 5 and 6 were the most resistant to moisture damage as their IDT strength actually improved with conditioning. Using Tukey's HSD for the asphalt binder/conditioning interaction, only PMA was significantly affected by conditioning, though this interaction manifested as an unanticipated strength gain with conditioning. Analysis of LS means showed that the limestone mixtures were significantly stronger than granite mixtures and that PMA mixtures produced a statistically significant strength gain compared to ARB mixtures.

### *4.2.4 Cantabro Loss*

The final test run on LMLC specimens was the Cantabro Loss test. This test was the second of two tests aimed at determining the effect of the laboratory conditioning using the MIST device. As in the IDT strength test, three unconditioned (Pre-MIST) and three moisture-conditioned (Post-MIST) compacted specimens were tested. Specimens were placed in the LA abrasion test drum at 20±2°C and rotated 300 times at a rate of 30 to 33 rotations per minute according to ASTM 6931. Figure 26 shows a comparison of specimen condition before and after testing. The mass before and after testing was recorded and the average Cantabro Loss value, before and after conditioning, was calculated for each mixture.


**FIGURE 26 Cantabro Loss Specimens – Before and After Testing.**

The ANOVA model ($\alpha = 0.05$) was again used to examine test results. Gradation, asphalt binder, and conditioning were considered as main effects and all possible two-way effects between them were considered. RMSE of all 36 observations was 2%. and results are plotted in Figure 27. The graph in Figure 27 provides a comparison of Cantabro Loss values before and after conditioning. From the data, mixture 1 and 2 were statistically better performing mixtures than mixtures 3 through 6, with mixture 2 outperforming all mixtures. Mixture 3 was the *least* durable mixture, with an average loss after testing of 13.3%. Conditioning was not a statistically significant factor, meaning that the chosen conditioning protocol did not impact the outcome of the Cantabro Loss experiment. Figure 28 presents a comparison of the Cantabro Loss values for the PMA and ARB mixtures, before and after MIST conditioning. ANOVA results show that asphalt binder type *was* a significant factor and asphalt mixtures made with ARB were the most durable, with an LS Means Cantabro Loss value 48% lower than

PMA. Additionally, aggregate type statistically influenced results as limestone mixtures out performed granite mixtures by 24%.

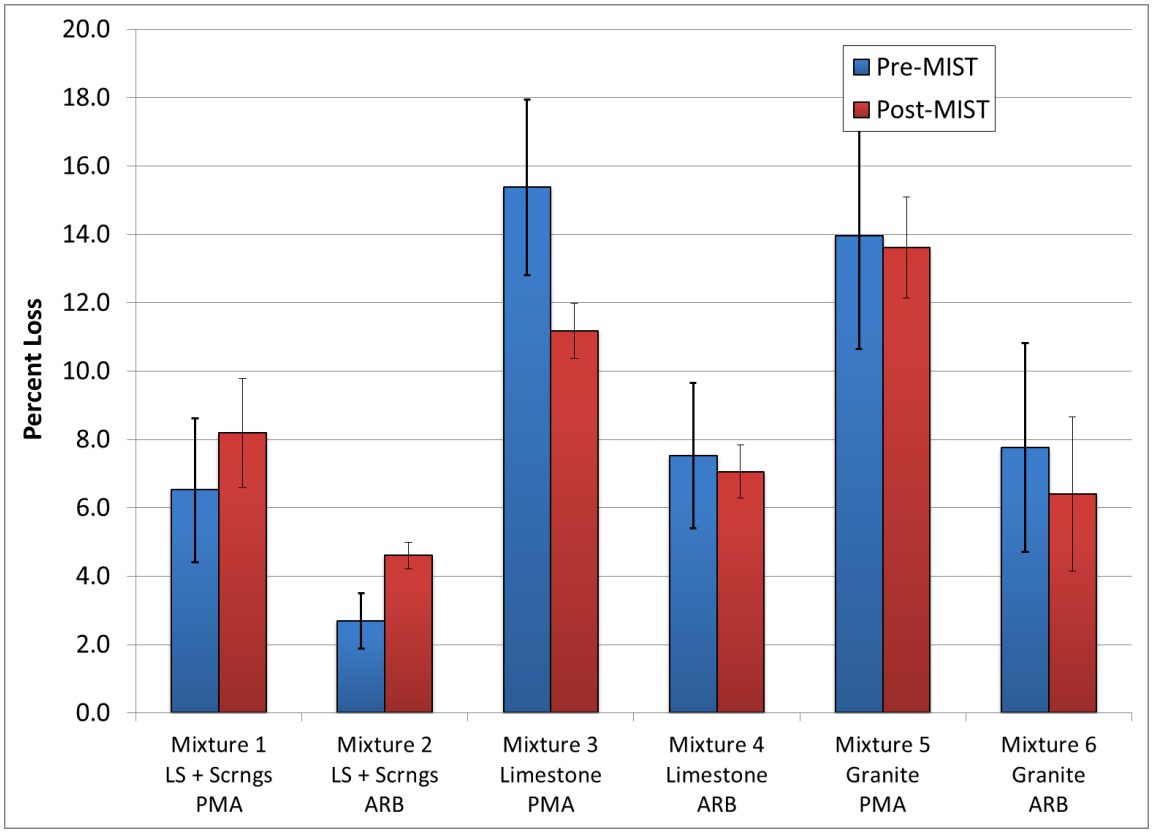


**FIGURE 27 Cantabro Loss – Pre-MIST vs. Post-MIST.**

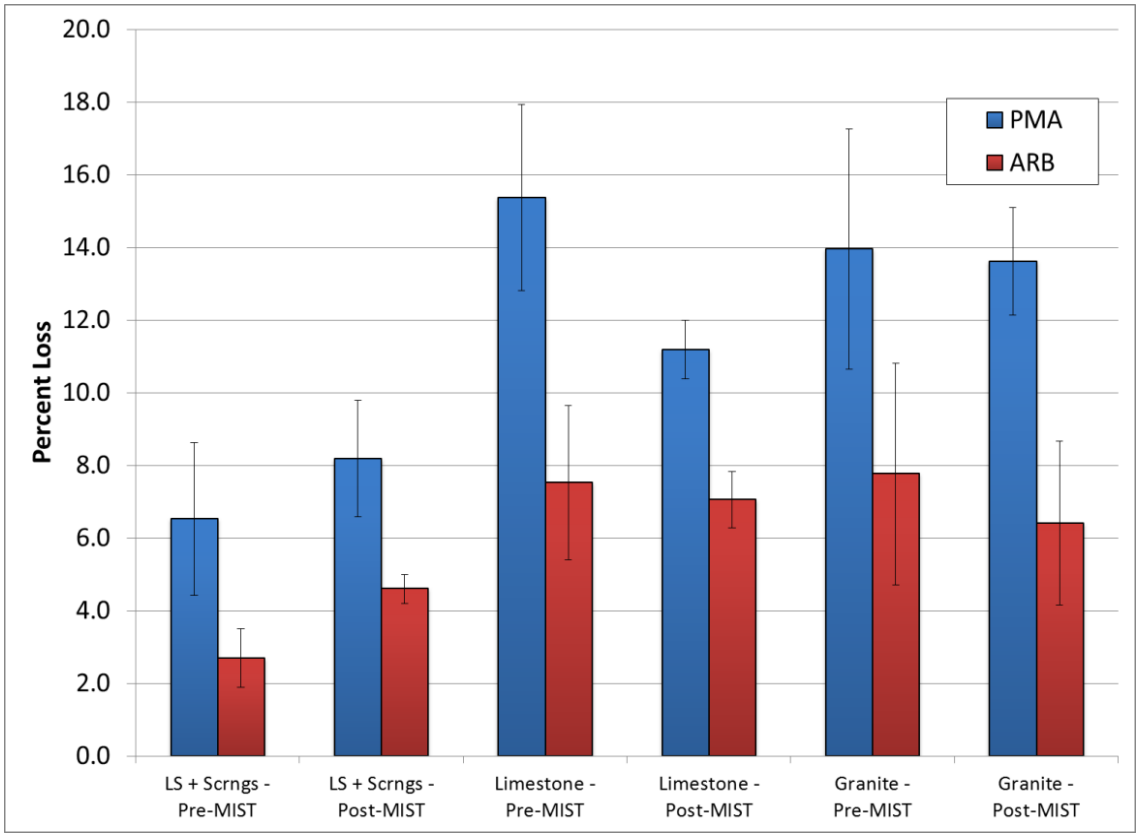


**FIGURE 28 Cantabro Loss – PMA vs. ARB.**

### 4.3 Moisture Conditioning Protocol – MIST Analysis

The intent of this research was to evaluate and recommend a laboratory conditioning protocol to apply to PFC mixtures after which laboratory results correlated well with field durability data and thus could be used to predict performance in the field. An integral part of that approach was the quality of the laboratory conditioning protocol. As discussed previously, the MIST was chosen to moisture condition LMLC specimens. The MIST had been shown in several studies (*21; 30-32*) to provide accelerated damage from moisture conditioning and to be a viable alternative to the traditional AASHTO T283 test. The MIST parameters of 1,000 cycles, 60°C, and 276 kPa were chosen from

previous experience with PFC which suggested the 3,500 cycles required in ASTM 7870 would destroy the open-graded asphalt mixture.

Based on the experimental results from the IDT and Cantabro Loss tests, moisture conditioning with the MIST did not produce the desired level of moisture damage. In the IDT test, five of six specimens had a TSR above 100% suggesting that the MIST protocol actually made the specimens stronger. In fact, statistical analysis showed that moisture conditioning was a significant factor, but opposite to that of the research hypothesis. For the Cantabro Loss test, four of six specimens showed a decrease in Cantabro Loss percentage, again suggesting that the asphalt mixtures *improved* with moisture conditioning. This result is counter to the existing body of research. In addition, HWTT test results showed that all six asphalt mixtures never reached the SIP and thus were likely not susceptible to moisture damage. This, combined with the lower-than-recommended number of MIST cycles, likely caused the selected MIST protocol to insufficiently damage the asphalt mixtures.

### *4.3.1 MIST Conditioning Protocol Study*

To investigate the effect of changing the MIST conditioning protocol, a small study was run on mixture 5 LMLC specimens using the IDT strength test. Results of this study are summarized in Table 17. ASTM 7870 recommends testing of MIST conditioned specimens within six hours of completing the conditioning protocol. That procedure was not followed during the previous research due to the porous nature of PFC mixtures and

the need to have dry specimens for the Cantabro Loss test. Two additional MIST conditioning protocols were run with the IDT test run immediately after the standard two hour wet conditioning at 25°C.

**TABLE 17 MIST Protocol - Sample Study Results**

| Conditioning | IDT, kPa | TSR |
|---|---|---|
| **Unconditioned** | 529 | - |
| **MIST Conditioned** | | |
| 1000 Cycle_72hr Dry[a] | 868 | 164% |
| 1000 Cycle_Wet | 602 | 114% |
| 5000 Cycle_Wet | 562 | 106% |

[a] Procedure used for this research

The results of the small study on the MIST protocol show that for each sample the wet testing greatly reduced IDT strength as compared to the dry testing and that the 5000 MIST cycle specimen had a lower IDT strength than the 1000 MIST cycle specimen. However, all three MIST conditioned specimens *still* had a TSR above 100% indicating that the specimens grew stronger with moisture damage. These asphalt mixtures clearly have a higher than normal resistance to moisture damage, and further research is needed to investigate adequate moisture conditioning protocols for low moisture susceptibility asphalt mixtures.

*4.3.2 Water Retention in MIST Conditioned Specimens*

The very nature of testing for moisture susceptibility requires that compacted specimens be submerged in water. As discussed in the previous section, the IDT and Cantabro Loss experiments tested compacted specimens after they had been subjected to moisture and then dried. As water is incompressible, it was desirable to remove all residual water after moisture conditioning. To determine the amount of water remaining in a specimen after drying, the mass of specimens was tracked throughout the conditioning process. Analysis of the data revealed that after moisture conditioning *and* air drying for 48-72 hours, Cantabro Loss specimens retained an average of 0.9% of specimen weight (about 35 grams) of additional water and IDT specimens retained an average of 0.6% of specimen weight of additional water (about 15 grams). As an example, a Cantabro Loss specimen had a mass of around 3900 grams and a volume of approximately 2040 $cm^3$. At 20% air voids, the volume of air voids in the compacted specimen was about 410 $cm^3$. 35 grams of water occupies 35 $cm^3$ of space, therefore, after air drying, about 8% of the air voids in the Cantabro Loss specimens were still filled with water. To remove this additional water the CoreDry device was used to achieve constant mass according to ASTM D 7227. This procedure reduced retained water to 2% and 3% of specimen weight for IDT and Cantabro Loss specimens, respectively. At 2% water, approximately 2.5% of specimen air voids are filled with water. This additional water was likely not enough to significantly impact the IDT strength or Cantabro loss of compacted specimens.

### 4.4 Significance of Results

Table 18 provides a summary of all laboratory tests used during this research which contribute data or parameters used to characterize the moisture susceptibility of individual asphalt mixtures. Each test is presented with the value or range of the desired result and an explanation of the effect that result has on the component or the asphalt mixture.

**TABLE 18 Properties Desired for Moisture Resistant Asphalt Mixtures**

| Component/Test | Desired Result | Effect of Desired Result |
|---|---|---|
| AIMS | High Angularity<br>High Texture<br>Low Sphericity | Better mechanical bonding |
| G-R Parameter | G-R < 180 kPa | Lower G-R indicates less likely to crack and/or ravel |
| SFE | High ER Values | More work required for water to displace asphalt binder = less thermodynamically favorable |
| IDT | High TSR | Less susceptible to moisture damage |
| Cantabro Loss | Low % Loss | Less susceptible to moisture damage |
| HWTT | Low Rut Depth<br>High/No SIP | Better rutting resistance<br>Less susceptible to moisture damage |
| Permeability | High k-value | Water/Moisture drains faster |

Based on the properties shown in Table 18, Tables 19 and 20 summarize the results from both observational and statistical analysis of the full regimen of component material and

performance tests. This data has been presented throughout the preceding sections and is presented here for comparative analysis. A review of the summary data shows variability between the best performer from each test and the proposed moisture sensitivity of the corresponding asphalt mixture. The component material test results in Table 19 indicate that an asphalt mixture made with PMA would produce a less moisture susceptible asphalt mixture.

**TABLE 19 Analysis Summary of Component Material Testing**

| Test | Component | Best Material(s) | Impacted Mixtures | Reason |
|---|---|---|---|---|
| AIMS | Aggregate | Granite | 5, 6 | Slightly higher texture - better mechanical bonding |
| G-R Parameter | Asphalt Binder | PMA | 1, 3, 5 | Slower advance of G-R toward early raveling |
| SFE | Combinations | Limestone+PMA | 1, 3 | Least moisture susceptible combination |

An examination of the performance test results in Table 20 shows a great deal of variability in outcome. The best performer in the IDT test, mixture 3, was the worst performer in the Cantabro Loss test. In addition, PMA asphalt mixtures outperformed ARB asphalt mixtures in the IDT test, but the opposite was true for the Cantabro Loss test where ARB outperformed PMA. The HWTT results would appear to have some correlation with the IDT data in terms of which gradation performed better than others,

but the HWTT actually revealed that none of the asphalt mixtures were moisture susceptible.

**TABLE 20 Analysis Summary for Performance Tests**

| Test | Gradation | | Mixture | | Asphalt Binder | | MIST | Aggregate |
|---|---|---|---|---|---|---|---|---|
| | Best | Worst | Best | Worst | Best | Worst | | |
| IDT | B | A/C | 3 | 6 | PMA | ARB | S.[b] | Limestone |
| Cantabro | A | B/C | 2 | 3 | ARB | PMA | N.S.[a] | Limestone |
| HWTT | B/C | A | 3/4/5 | 1/2 | N.S.[a] | | - | N.S.[a] |
| Permeability | A/B | C | 1 | 5/6 | N.S.[a] | | - | Granite |

Gradation A: Limestone with Screenings (Mixtures 1/2)
Gradation B: Limestone (Mixtures 3/4)
Gradation C: Granite (Mixtures 5/6)

[a] N.S. = Factor *not* significant

[b] S. = Factor significant

### 4.5 Correlation to Field Performance

The results of the component material and performance tests were compared with the field performance of mixtures 1, 2, and 3 to recommend a testing protocol that correlates well with the field data. Recall that the "good" performing mixtures that exhibited little to no raveling in the field were mixtures 1 and 2. These asphalt mixtures were made with the finer limestone gradation A, and both PMA (mixture 1) and ARB (mixture 2) asphalt binder. Mixture 3 was made of limestone as well, but used the coarser gradation B. In addition, mixture 3 used ARB asphalt binder. From the component material tests, the G-R parameter and SFE both recommended the superior performance of the PMA

mixtures and should be considered as one tool to contribute to the overall recommendation of the moisture susceptibility of an asphalt mixture.

Considering the field performance data when studying the outcomes of the performance tests yields a strong correlation between the Cantabro Loss test data and the field performance of the mixtures. The Cantabro Loss test revealed that mixtures 1 and 2 were superior performers and that mixture 3 was the least durable. This was the only test that correlated well with the field data revealing a strong statistical significance for the low durability of mixture 3. Therefore, the Cantabro Loss test is recommended to predict the moisture susceptibility of PFC asphalt mixtures.

Unfortunately, due to the lack of moisture damage from the MIST protocol, the correlation with performance test data and field performance must be considered with laboratory moisture conditioning having a minimal impact on asphalt mixture performance.

# 5. CONCLUSIONS AND RECOMMENDED FUTURE RESEARCH

The objective of this study was to recommend laboratory testing and conditioning protocols to induce PFC asphalt mixture degradation and simulate field conditions. These protocols are intended to be used in forensic analysis or to evaluate PFC mix design procedures. Morphological and physiochemical properties of asphalt mixture component materials were examined to reveal the component materials' propensity for moisture susceptibility. Volumetrics, binder stiffness, aggregate morpholgy, and SFE were evaluated. LMLC specimens of six asphalt mixtures were tested using the HWTT, and a single conditioning protocol was used to evaluate the effect of the conditioning protocol on IDT strength and Cantabro Loss. The following specific conclusions can be made based on this study:

1. PFC specimens expand in both the vertical and diametral directions when extracted from SGC molds. This phenomenon occurs even when specimens are extracted into molds. This expansion varies from 0.5 to 1.5 millimeters and if unaccounted for will yield compacted specimens with air voids 1-2% higher than expected.

2. Comparison of the number of gyrations required to make LMLC specimens revealed that mixtures 5 and 6 required a considerably higher compaction effort to meet the specified air void content of 20%. This indicates that standard field

compaction may lead to higher than specified air voids in these mixtures leading to a greater susceptibility to moisture damage and raveling.

3. G-R parameter values with aging indicate that the ARB asphalt binder has a faster advance to early raveling than PMA asphalt binder. This is an indication that ARB may age faster in the field and that ARB asphalt mixtures may be more susceptible to raveling as they age.

4. Comparison of the angularity, texture, and sphericity values determined by the AIMS indicates that there is no significant difference in the morphological properties of the limestone and granite aggregates used in FDOT PFC mixtures. These similar properties would seem to exclude aggregate morphology as a factor in the moisture susceptibility of asphalt mixtures made using these two aggregates.

5. The Cantabro Loss test is the best predictor of the durability of PFC mixtures as determined by field performance. While moisture conditioning was not a statistically significant factor in the test results, the average Cantabro Loss values for mixtures 1, 2, and 3 correlated well with the observed field performance of those mixtures. The IDT and HWTT results did not correlate with field performance.

6. The ASTM 7870 MIST conditioning protocol is not recommended for moisture conditioning of PFC specimens. As discussed by Little and Jones (*18*), this is likely due to the cohesive strength and healing ability of modified asphalt binders.

Based on this study, the following recommendations for future research can be made:

1. The MIST conditioning protocol for this study did not induce sufficient moisture damage. A small study was run to assess the effect of changing the number of MIST cycles which showed that as the cycles increased, the TSR of IDT specimens remained above 100%. Further research is required to understand the strengthening of modified asphalt binder in PFC using the MIST device. The feasibility of using the MIST device to provide accelerated moisture conditioning should also be examined.

2. In this study it was found that in order to achieve target air voids for all six asphalt mixtures, different levels of compaction were required. This was reflected in the number of gyrations each asphalt mixture required to reach the specified height. Additional research is required to determine the effect on PFC mixture moisture susceptibility when controlling the level of compaction.

3. The permeability of the asphalt mixtures was moderately dependent on the number of gyrations used to compact the specimens. Additional research into the effect of gyration level on the post-compaction gradation of asphalt mixtures and its impact on the permeability of PFC is recommended.

4. This study used the SFE of the component materials to evaluate the moisture susceptibility of the aggregate-asphalt binder combinations. There was a moderate correlation between the results and field observations. However, future research should examine the effect of the larger film thickness of PFC mixtures on moisture susceptibility and whether it is controlled by adhesive failure at the aggregate-asphalt binder interface or cohesive failure within the asphalt binder.

5. The two aggregates used in this study had similar angularity, texture, and sphericity values as determined by the AIMS. Due to the insignificant differences between these two aggregates, the morphological properties of the aggregate were not a factor in the moisture susceptibility of the asphalt mixtures. Future research using aggregates with differing angularity, texture, and sphericity values in PFC mixtures could reveal the effect of aggregate morphology on the moisture susceptibility of PFC mixtures.

## REFERENCES


1. Huber, G. *Performance Survey on Open-Graded Friction Course Mixes*. Synthesis of Highway Practice 284. Transportation Research Board, National Research Council, 2000.

2. Kandhal, P. S. *Design, Construction, and Maintenance of Open-Graded Asphalt Friction Courses*. Information Series 115. National Asphalt Pavement Association, 2002.

3. Cooley, L. A. *Construction and Maintenance Practices For Permeable Friction Courses*. NCHRP Report 640. Transportation Research Board of the National Academies, 2009.

4. Mo, L. T., M. Huurman, M. F. Woldekidan, S. P. Wu, and A. A. A. Molenaar. Investigation into material optimization and development for improved ravelling resistant porous asphalt concrete. *Materials & Design*, Vol. 31, No. 7, 2010, pp. 3194-3206.

5. Watson, D., A. Johnson, and D. Jared. Georgia Department of Transportation's Progress in Open-Graded Friction Course Development. *Transportation Research Record*, No. 1616, 1998, pp. 30-33.

6. Kandhal, P. S., and R. B. Mallick. Open Graded Asphalt Friction Course: State of Practice. *Transportation Research Circular*, No. E-C005, 1998.

7. Pavement Interactive. *Open Graded Friction Courses – Keeping an Open Mind*. http://www.pavementinteractive.org/2011/06/07/open-graded-friction-courses-keeping-an-open-mind. Accessed 24 August 2015.

8. Rand, D. Update on Permeable Friction Courses in Texas. In *Louisiana Transportation Conference*, Baton Rouge, LA., Jan 10, 2011.

9. Arámbula, E., C. K. Estakhri, A. Epps Martin, M. Trevino, A. de Fortier Smit, and J. Prozzi. *Performance and Cost Effectiveness of Permeable Friction Course (PFC) Pavements*. FHWA/TX-12/0-5836-2. Texas A&M Transportation Institute, Texas A&M University, College Station, TX, 2013.

10. Bennert, T., and L. A. Cooley. *Evaluate the Contribution of the Mixture Components on the Longevity and Performance of FC-5*. BDS15 977-01. FDOT, Center for Advanced Infrastructure and Transportation, Rutgers University, New Brunswick, NJ, 2014.

11. Molenaar, J. M. M., and A. A. A. Molenaar. *An Investigation into the Contribution of the Bituminous Binder to the Resistance to Raveling of Porous Asphalt*. 2nd Eurasphalt & Eurobitume Congress, Barcelona, Spain, Sep 20-22, 2000.

12. Hagos, E. T., A. A. A. Molenaar, M. F. C. Van De Ven, and J. L. M. Voskuilen. Durability Related Investigation into Porous Asphalt. In *The International Conference on Advanced Characterisation of Pavement and Soil Engineering Materials*, Athens, Greece, Jun 20-22, 2007, pp. 713-727

13. Von Quintus, H. L., J. Mallela, J. Jiang, and M. Buncher. Expected Service Life of Hot-Mix Asphalt Pavements in Long-Term Pavement Performance Program. *Transportation Research Record: Journal of the Transportation Research Board,* Vol. 1990, 2007, pp. 102-110.

14. Santucci, L. Minimizing Moisture Damage in Asphalt Pavements. *Pavement Technology Update, Institute of Transportation Studies,* University of California Berkeley, Berkeley, CA, Vol. 2, No. 2, 2010.

15. Hicks, R. G., L. Santucci, and T. Aschenbrener. Introduction and Seminar Objectives. In *Moisture Sensitivity of Asphalt Pavements: A National Seminar*, San Diego, CA, Feb 4-6, 2003, pp. 37-70

16. Kiggundu, B. M., and F. L. Roberts. *Stripping in HMA Mixtures: State-of-the-Art and Critical Review of Test Methods*. Report 88-02. NCAT, Auburn, AL, 1988.

17. Caro, S., E. Masad, A. Bhasin, and D. N. Little. Moisture Susceptibility of Asphalt Mixtures, Part 1: Mechanisms. *International Journal of Pavement Engineering,* Vol. 9, No. 2, 2008, pp. 81-98.

18. Little, D. N., and D. R. Jones. Chemical and Mechanical Processes of Moisture Damage in Hot-Mix Asphalt Pavements. In *Moisture Sensitivity of Asphalt Pavements: A National Seminar,* San Diego, CA, Feb 4-6, 2003, pp. 37-70

19. St. Martin, J., L. A. Cooley, and H. R. Hainin. Production and Construction Issues for Moisture Sensitivity of Hot-Mix Asphalt Pavements. In *Moisture Sensitivity of Asphalt Pavements: A National Seminar*, San Diego, CA, Feb 4-6, 2003, pp. 37-70

20. Arambula Mercado, E. *Influence of Fundamental Material Properties and Air Void Structure on Moisture Damage of Asphalt Mixes.* PhD Dissertation. Texas A&M University, College Station, TX, 2007.

21. Schram, S. *Ranking of HMA Moisture Sensitivity Tests in Iowa*. Report RB00-012. FHWA, Iowa Department of Transportation, 2012.

22. Solaimanian, M., J. Harvey, M. Tahmoressi, and V. Tandon. Test Methods to Predict Moisture Sensitivity of Hot-Mix Asphalt Pavements. In *Moisture Sensitivity of Asphalt Pavements: A National Seminar*, San Diego, CA, Feb 4-6, 2003, pp. 37-70

23. Epps, J. A., P. E. Sebaaly, J. Penaranda, M. R. Maher, M. B. McCann, and A. J. Hand. *Compatibility of a Test for Moisture-Induced Damage with Superpave Volumetric Mix Design*. NCHRP Report 444. TRB, National Research Council, 2000.

24. Aschenbrener, T., R. Terrel, and R. Zamora. *Comparison of the Hamburg Wheel-Tracking Device and the Environmental Conditioning System To Pavements Of Known Performance*. CDOT-DTD-R-94-1. Colorado Department of Transportation, 1994.

25. Bhasin, A., D. Little, K. Vasconcelos, and E. Masad. Surface Free Energy to Identify Moisture Sensitivity of Materials for Asphalt Mixes. *Transportation Research Record: Journal of the Transportation Research Board*, Vol. 2001, 2007, pp. 37-45.

26. Little, D. N., and A. Bhasin. *Using Surface Energy Measurements to Select Materials for Asphalt Pavement*. NCHRP Web-Only Document 104. Transportation Research Board of the National Academies, 2006.

27. Alvarez, A. E., A. Epps Martin, C. Estakhri, and R. Izzo. Evaluation of Durability Tests for Permeable Friction Course Mixtures. *International Journal of Pavement Engineering*, Vol. 11, No. 1, 2010, pp. 49-60.

28. Watson, D. E., K. A. Moore, K. Williams, and L. A. Cooley. Refinement of New-Generation Open-Graded Friction Course Mix Design. *Transportation Research Record: Journal of the Transportation Research Board*, Vol. 1832, 2003, pp. 78-85.

29. Putnam, B. J. *Evaluation of Open-Graded Friction Courses: Construction, Maintenance, and Performance*. FHWA-SC-12-04. SCDOT, Clemson University, Clemson, SC, 2012.

30. Chen, X., and B. Huang. Evaluation of Moisture Damage in Hot Mix Asphalt Using Simple Performance and Superpave Indirect Tensile Tests. *Construction and Building Materials*, Vol. 22, No. 9, 2008, pp. 1950-1962.

31. Zofka, A., M. Maliszewski, and A. Bernier. Alternative Moisture Sensitivity Test. In *The 9th International Conference "Environmental Engineering"*, Vilnius, Lithuania, May 22-23, 2014.

32. Weldegiorgis, M. T., and R. A. Tarefder. Towards a Mechanistic Understanding of Moisture Damage in Asphalt Concrete. *Journal of Materials in Civil Engineering,* Vol. 27, No. 3, 2015.

33. Birgisson, B., R. Roque, A. Varadhan, T. Thai, and L. Jaiswal. *Evaluation of Thick Open Graded and Bonded Friction Courses for Florida*. Report 4504-968-12. FDOT, University of Florida, Gainesville, FL, 2006.

34. *Flexible Pavement Design Manual.* Office of Design, Florida Department of Transportation. 2015.

35. Chopra, M. B., and R. Andre. *Effect of Asphalt Cement Deficiency on Open-Graded Friction Courses*. FM Number 403703. FDOT, University of Central Florida, Orlando, FL, 2000.

36. *Flexible Pavement Condition Survey Handbook.* State Materials Office, Florida Department of Transportation. 2015.

37. *Determining the Optimum Asphalt Binder Content of an Open-Graded Friction Course Mixture Using the Pie Plate Method.* Florida Department of Transportation. FM 5-588, 2014.

38. Masad, E. A. *Aggregate Imaging System (AIMS): Basics and Applications*. FHWA/TX-05/5-1707-01-1. TxDOT, Texas Transportation Institute, Texas A&M University, College Station, TX, 2005.

39. Gates, L., E. A. Masad, R. Pyle, and D. Bushee. *Aggregate Image Measurement System 2 (AIMS2): Final Report*. FHWA-HIF-11-030. Highways for LIFE Program Office, FHWA, Pine Instrument Company, 2011.

40. Alvarez, A. E., A. E. Martin, C. Estakhri, and R. Izzo. Determination of Volumetric Properties for Permeable Friction Course Mixtures. *Journal of Testing and Evaluation,* Vol. 37, No. 1, 2009, pp. 1-10.

41. *Measurement of Water Permeability of Compacted Asphalt Paving Mixtures.* Florida Department of Transportation. FM 5-565, 2015.

42. *Standard Practice for Moisture Conditioning Compacted Asphalt Mixture Specimens by Using Hydrostatic Pore Pressure.* American Society of Testing and Materials. ASTM D7870, 2013.

43. Yin, F., E. Arambula, R. Lytton, A. Martin, and L. Cucalon. Novel Method for Moisture Susceptibility and Rutting Evaluation Using Hamburg Wheel Tracking Test. *Transportation Research Record: Journal of the Transportation Research Board*, Vol. 2446, 2014, pp. 1-7.

44. Kim, Y. R., B. Underwood, M. Sakhaei Far, N. Jackson, and J. Puccinelli. *LTPP Computed Parameter: Dynamic Modulus*. FHWA-HRT-10-035. FHWA, Turner-Fairbank Highway Research Center, 2011.

45. Glover, C. J., R. R. Davison, C. H. Domke, Y. Ruan, P. Juristyarini, D. B. Knorr, and S. H. Jung. *Development of a New Method For Assessing Asphalt Binder Durability with Field Validation*. FHWA/TX-05/1872-2. TxDOT, Texas Transportation Institute, Texas A&M University, College Station, TX, 2005.

46. Rowe, G. M., G. King, and M. Anderson. The Influence of Binder Rheology on the Cracking of Asphalt Mixes in Airport and Highway Projects. *Journal of Testing & Evaluation*, Vol. 42, No. 5, 2014, pp. 1063-1072.

47. Cheng, D. X., D. N. Little, R. L. Lytton, and J. C. Holste. Surface Energy Measurement of Asphalt and its Application to Predicting Fatigue and Healing in Asphalt Mixtures. *Transportation Research Record: Journal of the Transportation Research Board*, Vol. 1810, 2002, pp. 44-53.